LBL-17463 c.2
Preprint

Lawrence Berkeley Laboratory

UNIVERSITY OF CALIFORNIA

Materials & Molecular Research Division

RECEIVED
LAWRENCE
BERKELEY LABORATORY

MAY 1 1984

LIBRARY AND
DOCUMENTS SECTION

Submitted to Chemical Society Reviews

SURFACE SCIENCE VIEW OF HETEROGENEOUS CATALYSIS: THE PAST, PRESENT AND FUTURE

G.A. Somorjai

March 1984

TWO-WEEK LOAN COPY

This is a Library Circulating Copy which may be borrowed for two weeks. For a personal retention copy, call Tech. Info. Division, Ext. 6782.

LBL-17463 c.2

Prepared for the U.S. Department of Energy under Contract DE-AC03-76SF00098

DISCLAIMER

This document was prepared as an account of work sponsored by the United States Government. While this document is believed to contain correct information, neither the United States Government nor any agency thereof, nor the Regents of the University of California, nor any of their employees, makes any warranty, express or implied, or assumes any legal responsibility for the accuracy, completeness, or usefulness of any information, apparatus, product, or process disclosed, or represents that its use would not infringe privately owned rights. Reference herein to any specific commercial product, process, or service by its trade name, trademark, manufacturer, or otherwise, does not necessarily constitute or imply its endorsement, recommendation, or favoring by the United States Government or any agency thereof, or the Regents of the University of California. The views and opinions of authors expressed herein do not necessarily state or reflect those of the United States Government or any agency thereof or the Regents of the University of California.

LBL-17463

SURFACE SCIENCE VIEW OF HETEROGENEOUS CATALYSIS: THE PAST, PRESENT AND FUTURE

By Gabor A. Somorjai

Materials and Molecular Research Division,
Lawrence Berkeley Laboratory
and
Department of Chemistry,
University of California,
Berkeley, California 94720

Surface Science View of Heterogeneous Catalysis: The Past, Present and Future

Gabor A. Somorjai

Department of Chemistry,
and
Materials and Molecular Research Division,
of the Lawrence Berkeley Laboratory
University of California, Berkeley

Abstract

Modern surface science determines the atomic structure, composition, and oxidation states of atoms on the catalyst surface along with the molecular structure and bonding of adsorbates. This molecular information has been correlated with the kinetic parameters of many catalyzed surface reactions, turnover rates, selectivity and activation energies. New catalysts have been developed and existing catalyst systems have been improved by systematic modifications that were suggested by molecular surface science. Catalysis science may now be applied to reactions important for energy conversion or for producing chemicals that have not yet been explored, as well as to other new areas.

INTRODUCTION

Practical catalysis that started during the last quarter of the 19th century took advantage of the development of thermodynamics that could determine the feasibility of chemical reactions. Then, an empirical search was made to find a suitable catalyst to drive the reaction toward thermodynamic equilibrium. In short order, several catalyst based chemical technologies have evolved that include the oxidation of SO_2, NH_3, the partial oxidation of methanol, benzene and naphthalene, the synthesis of ammonia and the synthesis of methanol and of other organic molecules from carbon monoxide and hydrogen[1]. The names of Ostwald, Sabatier, Mittash, and Haber comes to mind and it is my privilege to speak about catalysis in this city where much of the early history of catalysis was created.

While the important role surfaces play in heterogeneous catalysis was recognized, the investigations of surfaces was not an integral part of catalysis studies in the early days. Rather, surface chemistry became established with the development of the light bulb and the gas mask during the first quarter of the century[2]. Then, some of the greats of physical chemistry that include Polanyi, Langmuir, Bonhoeffer, Rideal, Roberts, Taylor and Farkas turned their attention to surface reactions and initiated studies to identify the elementary steps. Among them, perhaps Emmett was the leading spokesman for surface science studies of catalysts[3] (for ammonia synthesis and for the hydrogenation of carbon monoxide) by selective adsorption, and by his attempts to relate the adsorption properties of the surface to the performance of the catalyst (rates and selectivity).

I. Modern Surface Techniques and their Applications to Heterogeneous Catalysis

The modern era of catalysis began with the availability of techniques that could characterize the catalyst surface on the atomic scale, and then carry out reactions on these surfaces to correlate the reaction rates and selectivities with these molecular parameters. Many of these techniques have been developed through surface science over the last twenty years that could determine the atomic structure of clean surfaces and adsorbed monolayers of atoms and molecules, the surface composition, with less than 1% of a monolayer sensitivity[2], and the oxidation states of surface atoms. Table I lists some of the techniques that are used most frequently in surface chemical and catalytic reaction studies. The advantage of these is the need for very small areas in the range of 10^{-4} to 10^{-1} cm, for definitive studies[4]. The disadvantage is that they often require ultra-high vacuum ($\sim 10^{-8}$ torr) for definitive investigations of the surface, and they can be utilized for studies of external surfaces only.

In order to utilize the small area well characterized surfaces for catalytic reaction studies at high pressures, we developed a low-pressure high-pressure apparatus that is shown in Figure 1. The small area samples, often single crystals, or polycrystalline foils, after suitable surface characterization in ultra-high vacuum by LEED, AES, and other surface sensitive techniques, are enclosed in an isolation cell[5] that can be pressurized with the reactants. The sample is then heated to the reaction temperature and the products that form are analyzed by a gas chromatograph that is connected to the high pressure loop.

The high pressure reactor can be used in batch or in flow modes. The detection sensitivity of the gas chromatograph is high enough that a one square centimeter surface area is adequate to monitor the product distribution, as long as the reaction turnover rates over the catalysts are greater than 10^{-4} molecules per site per second. Using this high pressure low pressure apparatus we can carry out catalytic reactions under conditions that are virtually identical to those used in the chemical technology. We can then evacuate the high pressure cell, open it, and analyze the surface properties of the working catalyst in ultra-high vacuum using the various techniques of surface science. Then the isolation cell may be closed again and the high pressure reaction may be continued and again interrupted for surface analysis in vacuum. Using this apparatus we could show not only that the catalytic reactions can be readily investigated using small area single crystal surfaces, but that these surfaces can be used as model heterogeneous catalysts. Studies of the atomic structure and composition of the internal surfaces of high surface area catalysts like the zeolites, for example, require different techniques of modern surface science. Among them, solid-state NMR and EXAFS (extended X-ray absorption fine structure), and X-ray photoelectron spectroscopy (XPS) have been found particularly useful in studies of this class of catalysts in recent years.

Since my research utilized small area, mostly single crystal surfaces as model catalysts, this talk concentrates on the results that were obtained using such systems. Similar small area single crystal surfaces

were also used for studies of elementary surface reactions at low pressures[6], adsorption, rearrangements, surface diffusion and desorption, and the dynamics of gas surface collisions by the use of molecular-beam surface scattering[7]. Our catalytic reaction studies benefited greatly from these surface science studies.

When using model catalysts, it is essential to establish credibility to acertain that the rates of a variety of chemical reactions are similar or identical on these surfaces when compared with those on high surface area dispersed metal catalysts. We have found nearly identical reaction rates for the ring opening of cyclopropane on platinum[8], the hydrogenation of cyclohexene on platinum[9], and for the hydrogenation of carbon monoxide to methane on rhodium[10].

II. The Results of Molecular Studies of Catalytic Reactions on Model Catalyst Surfaces

A. Structure Sensitivity

Figure 2 compares the rates of ammonia production on three single crystal surfaces of body centered cubic iron at high pressures[11]. The (111) face is about 430 times more active than the closest packed (110) crystal face while the (110) face is 32 times as active as the (110) face. The rate limiting step in this reaction is the dissociation of N_2 and it appears that this process occurs with the near zero activation energy on the (111) iron surface, while there is a larger activation energy for the automization of N_2 on the other iron crystal surfaces. It has been proposed that the active site for breaking the very strong N_2 bond is a seven coordinated iron atom that is present in the second layer

under the surface. There is a theory being developed[12] that relates the concentration of nearly degenerate electron vacancy states, the density of whole states near the fermi level to the ability of a given site to break and make chemical bonds in a transient manner by charge fluctuations. The sites with of the largest number of nearest neighbors (highest coordination) have the highest density of electron hole states and thus they should be the most active during catalytic reactions. Unfortunately, they are located in the bulk and are not accessible to the incoming reactants. However, atoms in the second layer of an open surface structure are accessible, but are still surrounded by a large number of neighbors. These are then the most active sites in many catalytic reactions. While this theory will have to be tested further, and proven by careful experiments, the available experimental data on the structure sensitivity of catalytic reactions can be explained by it. Figure 3 shows the rate of ammonia formation from N_2 and H_2 over hexagonal close packed rhenium crystal surfaces[13]. Again, the open $(11\bar{2}0)$ crystal face is about 1000 times more active than the closest packed (0001) hexagonal surface, thus exhibiting a profound structure sensitivity that is even more pronounced then that on iron.

In addition to the flat, low Miller index surfaces, we also utilized high Miller index surfaces for studies of the conversion of hydrocarbons on platinum single crystal surfaces[14]. These surfaces exhibit ordered, stepped terrace arrangements where the terraces are of variable width, depending on the angle of the cut, and they are separated by periodic steps of usually one atom in height (Figure 4). The step periodicity,

as well as the step height can readily be determined by LEED studies[15]. These surfaces can be cut in such a manner that the steps also have a large concentration of kinks (Figure 5). Surfaces may have as much as 40% of their atoms in step sites and the kink concentration can reach 10%. As compared to this high concentration of line defects, point defects such as adatoms or vacancies, have very small concentrations (<1%) when in equilibrium with the bulk and with other surface defects. These steps and kinks are stable under the conditions of most catalytic surface reaction. Figures 4 and 5 show some of the stepped and kinked surfaces that were prepared. These surfaces exhibited very different reactivities as compared to the flat surfaces. Adsorption studies of hydrocarbons and carbon monoxide revealed preferential bond breaking at these defects sites. C-H and C-C bond breaking was readily detectable on stepped or kinked platinum surfaces upon adsorption of organic molecules, even at 300K at low pressures, while under the same circumstances, the (111) surface was unreactive[16]. Molecular beam studies of H_2/D_2 exchange of stepped surfaces showed 7 to 10 fold higher dissociation probability of the hydrogen molecule on a single scattering than on the flat (111) crystal face[17].

The test reactions that best demonstrate the structure sensitivity of hydrocarbon conversion reactions over platinum are the conversion of n-hexane and n-heptane to other organic molecules[18]. n-hexane may convert to benzene upon dehydrocyclization or to methyl cyclopentane by a cyclization reaction. These are shown in Figure 6. It may isomerize to branched butanes or undergo C-C bond breaking (hydrogenolysis) to

produce C_1-C_3 fragments, methane to propane. The first three of these reactions are desireable when the aim is to produce high octane gasoline, while the fourth reaction is undesireable as it leads to the production of gases of much less value as fuels. Figure 7 shows that the hexagonal (111) surface produces much more aromatic products than the square (100) crystal face. In fact, a stepped surface with (111) orientation terraces that are five atoms wide, is perhaps the best catalyst found so far to carry out the dehydrocyclization reaction[18,19]. Conversely, the (100) flat surfaces with the square unit cells are much better isomerization catalysts as shown in Figure 8, than the hexagonal crystal surfaces of platinum[20]. Thus, depending on the catalyst preparation, one may obtain superior dehydrocyclization or isomerization activity that is certainly well documented in the patent literature. The hydrogenolysis reaction[18,21] that is also shown in Figure 8 is most active on surfaces that contain a large concentration of ledge or kink sites. It is often necessary to poison these sites by the adsorption of sulfur or other strongly bound additives that bind more strongly to the ledge sites than to the other surface sites (step or terrace sites). This way the ledges cannot participate in hydrocarbon reactions because they are masked by the selective adsorption of additives while by the rest of the higher coordination surface sites remain clean and thereby active and selective.

B. <u>The Carbonaceous Deposit</u>

A catalytically active metal surface is always covered with a carbonaceous deposit[22]. By labeling the reactant organic molecules with ^{14}C isotope, the residence time of this carbonaceous layer can be monitored[23].

It is found that it is usually ten to fifty times larger than the turnover time for the catalytic hydrocarbon conversion reactions. This is shown in Figure 9 under the label of irreversible adsorption, along with the hydrogen to carbon ratio of this deposit. As the reaction temperature is increased, the deposit becomes more dehydrogenated, as its stoichiometry changes from C_2H_3 to C_2H, as determined by hydrogen thermal desorption and finally it looses a hydrogen and becomes graphitic[24]. While the metal surface retains its catalytic activity as long as the carbonaceous deposit contains hydrogen, it becomes completely inactive, poisoned in the presence of the graphitic overlayer. The sequential dehydrogenation of adsorbed organic monolayers with increasing temperature, can be readily demonstrated by temperature programmed thermal desorption studies. Figure 10 shows the evolution of hydrogen from adsorbed layers of C_2H_4, C_3H_6 and C_4H_8[24]. At well defined temperatures, hydrogen evolves at a maximum rate until complete dehydrogenation and graphitization of the remaining carbon occurs at the highest temperatures. LEED and HREELS studies reveal the structure of organic monolayers at each stage of chemisorption. At lower temperatures, less or equal to 300K, the organic molecules exhibit ordered molecular structures[25]. Figure 11 shows one of the ordered surface structures of benzene on the rhodium (111) crystal face[26] that was determined by LEED surface crystallography and Figure 12 shows the HREELS spectra of benzene and its deuterated form[27]. The C_{3v} symmetry is clearly compatible with the molecular structure shown in Figure 11 with the molecule lying with its π-ring parallel to the surface, and the center of the ring above a 3 fold hollow. Figure 13 shows the surface structures of chemisorbed ethylene, propylene and butene on the

platinum (111) crystal face[28]. These molecules form ethylidyne species upon adsorption near 300K with their C-C bond that is closest to the metal surface, perpendicular and alongated to a single C-C bond length. Similar ethylidyne structures have been found on other transition metal surfaces as well that include paladium, rhodium and nickel[29]. The carbon atom that binds the molecule to the metal prefers this 3 fold hollow site. Figure 14 compares the molecular structure of the ethylidyne molecule on the platinum (111) surface with the structures of ethylidyne containing trinuclear metal compounds. The symmetry, the bond distances and the bond angles in these clusters are very similar to the molecular structure of chemisorbed ethylene on the transition metal surface. This similarity indicates the predominance of localized bonding[30] of adsorbed surface species, an important conclusion in our scrutiny of the surface chemical bond[2].

Figure 15 shows the sequential change of the vibrational spectrum of chemisorbed C_2H_4 on the rhodium (111) crystal face as the temperature is increased[31]. The molecule decomposes and there is evidence for the presence of CH, C_2 and C_2H species on the surface in the spectra. Figure 16 shows schematically many of these species that were detectable by HREELS, not by LEED because these fragments are disordered) and also $-CH_3$ that has not been observed as yet[32]. It is believed that the location of these organic fragments is governed by the necessity of tetrahedral symmetry for the bonding of carbon atoms. That is, ≡CH fragments occupy 3-fold sites, with bonding to three metal atoms. $=CH_2$ fragments have two metal bonds at the bridge site and by analogy a $-CH_3$ fragment should have one metal bond and be localized at the top site[32]. If this is the desired bonding configuration of the various fragments,

it explains the mechanism by which the three fold strongly binding sites are freed up by successive hydrogenation of the fragments, and become available to the next incident molecule.

The alkylidine molecules are present only under conditions of catalyzed reaction at low temperatures as they decompose at about 400K on most transition metal surfaces. This restricts their importance, by and large, to hydrogenation reactions which, having low activation energies, may proceed well below 400K. Recent studies of C_2H_4 hydrogenation over platinum and rhodium crystal faces indicates[33] that it occurs on top of the ethylidine layer that remains ordered, and stable as its residence time is much longer than the turnover time needed for C_2H_4 hydrogenation to C_2H_6.

During other catalyzed hydrocarbon reactions that occur at an appreciable rate only at higher temperatures, the organic fragments are the permanent fixtures on the active metal surface during the reaction. Their main role appears to be hydrogen transfer to the adsorbed reaction intermediates[34] as the C-H bonds retain the hydrogen more easily than the bare transition metal surface. H-D exchange studies using pre-deuterated fragments or reactants indicate that the rate of H-D exchange is at least an order of magnitude faster than the turnover rate of most hydrocarbon conversion reactions. Thus the hydrogen atom in the C-H bonds of the strongly held organic fragments are readily transferred to the adsorbed intermediates, while the carbon atoms do not exchange easily.

Fortunately not all of the metal sites are covered with the organic fragments although AES studies indicate that more than a monolayer of carbon is

present on the metal surface under catalytic reaction conditions during hydrocarbon conversions. We can titrate the remaining bare metal sites by the chemisorption of carbon monoxide at low pressures, which under the same conditions does not adsorb on the carbonaceous deposit. Figure 17 shows the fraction of the bare metal surface (θ/θ_0) CO that is present after the reaction where θ_0 is a concentration of chemisorbed CO on the initially clean metal surface before the reaction[22]. About 5 to 20% of the platinum is uncovered, the bare metal area decreasing with increasing reaction temperatures. Of course, at higher hydrogen pressures (all hydrocarbon conversion reactions are carried out in the presence of excess hydrogen) the fraction of uncovered metal increases.

From these studies a molecular model of the working platinum catalyst can be constructed and shown in Figure 18. There are bare metal islands whose structure is determined mostly by the catalyst fabrication[22]. The incident reactant molecules adsorb and undergo chemical rearrangements on these metal islands. Then, the adsorbed intermediates diffuse onto the carbonaceous deposit, pick up one or more hydrogen, and desorb as the products. Once the carbon deposit lost all its hydrogen and becomes graphitic, hydrogen transfer that is an important part of catalytic reactions can no longer occur and the catalyst surface becomes inactive.

C. <u>The Oxidation State of Surface Atoms</u>

There are several experimental studies published in recent years that indicate the importance of oxidation states other than the zero valent metallic state for catalyzed reactions. During the hydrogenation

of carbon monoxide over rhodium, rhodium was reported to yield predominantly C_2 oxygenated products, acetaldehyde and acetic acid, when prepared under appropriate experimental conditions[35]. Our studies using unsupported polycrytalline rhodium foils have detected mostly methane along with small amounts of ethylene and propolene under very similar experimental conditions. This product distribution was identical to that obtained by Vanice over supported rhodium catalysts along with the activation energies for methanation about 24 kcal per mole that we both found[10]. It appears that most of the organic molecules form following the dissociation of carbon monoxide, by the rehydrogenation of CH_x units in the manner similar to alkane and alkene production from CO/H_2 mixtures over other more transition metal catalysts (iron, ruthenium, and nickel). However, when rhodium oxide (Rh_2O_3), was utilized as a catalyst, large concentrations of oxygenated C_2 or C_3 hydrocarbons were produced including ethanol, acetaldehyde and propionaldehyde[35]. Furthermore, the addition of C_2H_4 to the CO/H_2 mixture yielded propionaldehyde indicating the carbonylation ability of Rh_2O_3. Under similar experimental conditions over rhodium metal, C_2H_4 was quantitatively hydrogenated to ethane and carbonylation activity was totally absent. Clearly, higher oxidation state rhodium ions are necessary to produce the oxygenated molecules. Unfortunately, Rh_2O_3 reduced rapidly in the CO/H_2 mixture to the metallic state with drastic alteration of the product distribution from oxygenated hydrocarbons to methane. In order to stabilize the rhodium ion, lanthanum rhodate ($LaRhO_3$) was prepared by incorporating Rh_2O_3 into La_2O_3 at high temperatures[36]. Over this stable catalyst, the formation of oxygenated

products from CO/H_2 mixtures predominated. The marked change of selectivity in CO/H_2 reactions upon alteration of the oxidation state of the transition metal is due largely to the change of heats of adsorption of CO and $D_2(H_2)$ as the oxidation state of the transition metal ion is varied[36]. This is demonstrated in Figure 19. The CO adsorption energy is decreased upon oxidation while the heat of adsorption of D_2 is increased. This in turn changes the relative surface concentrations of CO and H_2. In addition, the metal is primarily active for hydrogenation and CO dissociation, while the oxide can perform carbonylation and has reduced hydrogenation activity. As shown in Figure 19, the active $IaRhO_3$ catalyst seems to have both rhodium metal and rhodium ion sites as indicated by the presence of several thermal desorption peaks of CO and H_2 to provide both optimum carbonylation as well as hydrogenation activity so necessary to obtain C_2 or C_3 oxygenated hydrocarbon molecules.

One of the difficulties in preparing selective catalysts for hydrocarbon conversion is the poor thermodynamic stability of higher oxidation states of transition metal ion in the reducing reaction environment. It appears that the strong metal support interaction that permits the incorporation of the high oxidation state transition metal ion into the supporting refractory oxide or sulfide crystal lattice often provides for the kinetic stability of the desired oxidation state, as long as the catalytic reaction temperatures are appreciably below the decomposition temperature of the binary oxide so prepared.

Another example of the importance of the changing oxidation state of transition metal ions at the surface is shown by the catalytic cycle leading to the photocatalyzed dissociation of water on strontium titanate, $SrTiO_3$ surfaces[37]. This is shown in Figure 20. The oxide surface is completely hydroxylated in the presence of water, and the titanium ions are in the Ti^{4+} oxidation state. When the surface region is irradiated with light of 3.1eV or larger energy, electron-hole pairs are generated. The electron is utilized to reduce the Ti^{4+} to Ti^{3+} formal oxidation state[2]. The electron vacancy induces charge transfer from the hydroxyl group that produces OH radicals that dimerize to H_2O_2 and splits off oxygen that evolves. The reduced Ti^{3+} containing surface can now adsorb another water molecule that acts as an oxidizing agent to produce Ti^{4+} again and a hydroxylated surface, evolving hydrogen in the process[38]. Clearly, changes of oxidation states of transition metal ions are frequently indispensible reaction steps in catalytic processes[39].

We have thus identified several of the molecular ingredients of heterogeneous catalysis. Models that emphasize the importance of the surface structure of catalysts for selectivity, the presence and involvement of organic fragments in HC conversion reaction and the need for various oxidation states of surface atoms to obtain desired reaction products are not new to the literature of catalysis. However, to establish direct correlation between these molecular parameters and the catalytic behavior eluded the practitioners of catalysis in the past. Surface science provided the tehniques for determination of the atomic structure, composition and oxidation state of surface atoms, and adsorbed molecules

in the monolayer and when combined with studies of the kinetic parameters of catalytic reactions (rates, selectivities, activation energies) the all important correlations between the molecular ingredients on the catalyst surface and the high pressure catalytic reaction behavior could be established.

As a result of these and many other similar studies using model or high surface area catalysts, catalysis is being converted from art to science. From the point of view of catalyst based industries, this conversion signals the advent of high technology, that is, when the development of the technology is science driven, and the rate of the development depends on the advances made by catalysis science. This then provides the opportunity to build or design new catalysts. Perhaps the first two high technology catalysts are the catalytic converter that is used on automobiles in the United States and the new generation of zeolites with high silicon to aluminum ratio compositions. Their rapid development could not have been possible without the application of modern surface science.

D. Building of New Catalysts

By giving the examples of surface and catalytic studies on well characterized systems, one can demonstrate the understanding that could be achieved on the molecular ingredients of important catalytic systems. We now can now utilize this understanding the build better systems by alteration of their structure or their state of surface charge. Below, we discuss two examples of deliberate catalyst modifications: the effect of gold on transition metal catalysis and the effects of the potassium on transition metal catalysts.

1. The Effect of Gold on the Selectivity and Activity of Platinum Catalysts

The influence of gold on hydrocarbon conversion catalysis by platinum has been studied by condensing Au on Pt crystal surfaces[40]. Gold forms epitaxial layers on Pt and upon heating it forms an alloy in the near surface region. This Au-Pt alloy has a markedly different selectivity[41] and activity for the conversion of n-hexane to other hydrocarbons as shown in Figure 21. The isomerization rate goes up as compared to that on clean Pt while the hydrogenolysis and dehydrocyclization rates are reduced exponentially with increasing gold concentration. This remarkable selectivity and activity alteration can be explained by a change of structure of the Pt(111) surface induced by gold alloying. By substitution of a gold atom the high coordination 3-fold Pt sites are eliminated much faster than the two fold and one fold bridge and top sites. This is commonly called the ensemble effect. As a result, the chemistry that requires the adsorption of molecules and surface intermediates at the 3-fold sites is eliminated while the chemical reactions that require adsorption at bridge or top sites are not attenuated. While subtle electronic changes may also occur at the alloy surface sites, most of the results can be rationalized by this selective high coordination site elimination model.

Similar observations were reported by Boudart et al. for the production of water from H_2 and O_2 over Pd-Au alloy surfaces[42]. Small amounts of gold increased the rate of this reaction by fifty fold.

It should be noted that gold is a very poor catalyst for both of these reactions. Nevertheless, its presence as an alloying constituent can beneficially influence the selectivity and the reactivity of transition metal catalysts.

Bimetallic alloys are frequently used for hydrocarbon conversion reactions instead of single component metal catalysts. In addition to often superior selectivity they maintain their activity at higher temperatures and deactivate slower. Alloying appears to slow down the rate of graphitization of organic fragments that are ever present on the transition metal catalyst surfaces by perhaps limiting the island size of these carbonaceous deposits.

2. The Effect of Potassium on the Bonding and Reactivity of Carbon Monoxide and Hydrocarbons.

Potassium has a high heat of adsorption when present in low coverages on transition metal surfaces (Figure 22). Simultaneously it also reduces the work function of the transition metals indicating large charge transfer between the metals[43]. A model that assumes that potassium is ionized when adsorbed on the transition metal surface explains these results. As the potassium concentration increases the charged species repell each other and depolarization occurs; the potassium layer becomes metallic and its heat of adsorption approaches rapidly the heat of sublimation of potassium metal.

Potassium has a strong influence on the heat of adsorption of CO on transition metal surfaces[44]. This is shown in Figure 23. In the absence of potassium, CO desorbs at a maximum rate from the Rh(111) surface at 400K. However, when co-adsorbed with 50% of a monolayer of potassium, it desorbs at 600K indicating a ∿12 kcal increase of its binding energy. The HREELS spectra of CO on Pt(111) also exhibits major changes[45] that are shown in Figure 24. In the absence of CO two well defined CO stretching frequencies are detectable that are associated with CO at a top and at a bridge site adsorbed with its CO bond perpendicular to the surface. As

the potassium is added to the Rh surface CO shifts to the bridge site and its stretching frequency decreases by more than 300 cm^{-1}. This corresponds to a gradual change of bond order with increasing potassium coverage from 2 to 1.5. This indicates that the electron transferred from the potassium to the transition metal density of states can populate the antibonding molecular orbitals of CO, thereby weakening the C-O bond. Simultaneously the metal carbon bond is strengthened as charge density in this bonding orbital must increase.

Potassium is often used as a beneficial additive to transition metal catalysts utilized for the hydrogenation of carbon monoxide. Its presence increases the molecular weight of hydrocarbon products as expected if the dissociation rate of carbon monoxide is enhanced.

Potassium however is a non-selective poison for hydrocarbon reactions on platinum surfaces[46]. The reason for this is revealed in recent surface studies. The presence of potassium increases the activation energy for the breaking of C-H bonds that is an important step in most hydrocarbon conversion reactions. This is shown in Figure 25. Thus, the surface residence time of the molecules increase that reduces the catalytic turnover rates.

There is little doubt that potassium influences the catalytic reaction by charge transfer, that is, by electronic changes. It has large effects on some molecules when coadsorbed with them (CO, N_2) and virtually no effects on others (NO, PF_3)[47]. It would be of value if we could predict by the use of theoretical guidance whether charge transfer between the molecular orbitals of adsorbates and the charge density that is altered by the adsorption of potassium on the transition metal surface could or could not take place.

E. New Directions of Catalysis Science for the Future

One of the most promising new directions of catalysis science is as old as Ostwald's studies of ammonia oxidation. Let us use the thermodynamic viewpoint again and find catalysts for important reactions that have not been investigated in detail before. There are many important reactions of small molecules that include CO_2, CH_4, H_2 and N_2, that may be investigated. Figure 26 shows the free energy changes associated with several reactions of these molecules.

The reaction of carbon with water to produce CH_4 and CH_2 is thermoneutral[48]. This process represents a desireable alternative for the gasification of carbon solids (coal, biomass) with water to the production of CO and H_2, a very endothermic reaction indeed[49]. The partial oxidation of methane to methanol and to formaldehyde should be feasible by suitable catalyst surfaces[50]. The oxidation of nitrogen to nitric acid in the aqueous phase is thermodynamically feasible and should be investigated for nitrogen fixation. While CO_2 hydrogenation is feasible its dissociation to CO and oxygen requires the input of excess energy. Indeed the photocatalyzed dissociation of both CO_2 and H_2O provide opportunities for solar energy conversion to fuels or chemicals that can be stored[51]. These reactions could all be carried out by innovative application of catalysis science, and they are needed because we need new feedstocks for fuels as well as for chemicals for the future. These studies provide ample opportunities for exciting new discoveries in the field of catalysis science in the near future.

Another important area of catalysis science is the catalysis of excited state molecules. Catalysis almost always utilizes molecules in their thermodynamic ground states. Even when endothermic reactions are

carried out, energy is always employed in the form of heat that assures, by and large, that thermodynamic equilibrium exists in the ground state configuration. However, using lasers and plasmas, it is possible to create large populations of molecules in their electronic or vibrational excited states. Their surface reactions are very likely to occur along reaction channels that are different from that in their ground state to yield new reaction products and perhaps improve selectivity.

It is my hope that the field of catalysis will be broadened to embrace many other areas of physical sciences that have not been viewed from a catalytic perspective. Catalysis of phase changes is one of them. It is important to learn how to catalyze crystal growth, evaporation or sintering (densification).

One of the frontiers of catalysis science lies at the solid-liquid interface. Newly developing surface science techniques[52] will permit the molecular level scrutiny of electrocatalysis and biological catalysis in the near future. Perhaps we might be able to explore the working on the molecular level of one of the most successful catalysts, the brain.

The future is indeed bright for catalysis science.

ACKNOWLEDGEMENT

This work was supported by the Director, Office of Energy Research, Office of Basic Energy Sciences, Materials and Chemical Sciences Division of the U.S. Department of Energy under Contract Number DE-AC03-76SF00098.

FIGURE CAPTIONS

Figure 1: Schematic representation of the experimental apparatus utilized to carry out the catalytic reaction rate studies on single crystal or polycrystalline surfaces of low surface area at low and high pressures in the 10^{-7} to 10^{+4} torr range.

Figure 2: The remarkable surface structure sensitivity of the iron catalyzed ammonia synthesis.

Figure 3: The structure sensitivity of ammonia synthesis on rhenium single crystal surfaces.

Figure 4: Structure of several high Miller Index stepped surfaces with different terrace widths and step orientations.

Figure 5: Surface structures of several high Miller Index surfaces with differing kink concentrations in the steps.

Figure 6: Skeletal rearrangement reactions of hydrocarbons catalyzed by platinum with high activity and unique selectivity. Depicted here are the several reaction pathways which occur simultaneously during the catalyzed conversion of n-hexane, C_6H_{14}. The isomerization, cyclization and aromatization reactions that produced branched or cyclic products are important in the production of high octane gasoline from petroleum naphtha. The hydrogenolysis reaction that involves breaking of C-C bonds yields undesirable gaseous products.

Figure 7: Dehydrocyclization of alkanes to aromatic hydrocarbons is one of the most important petroleum reforming reactions. The bar graphs shown here compare reaction rates for n-hexane and

Figure 7: (cont.) n-heptane aromatization catalyzed at 573 K, and atmospheric pressures over the two flat platinum single crystal faces with different atomic structure. The platinum surface with the hexagonal atomic arrangement is several times more active than the surface with a square unit cell over a wide range of reaction conditions.

Figure 8: Reaction rates are shown as a function of surface structure for isobutane isomerization and hydrogenolysis catalyzed at 570 K at atmospheric pressure over four platinum surfaces. The rates for both reaction pathways are very sensitive to structural features of the model single crystal catalytic surfaces. Isomerization of these light alkanes favored on the platinum surfaces that have a square (100) atomic arrangement. Hydrogenolysis rates are maximized when kinked sites are present at high concentrations as in the platinum (10,8,7) crystal surface.

Figure 9: Carbon 14 labeled ethylene C_2H_4 was chemisorbed as a function of temperature on a flat platinum surface with hexagonal orientation, Pt(111). H/C composition of the adsorbed species was determined from hydrogen thermal desorption studies. The amount of preadsorbed ethylene, which could not be removed by subsequent treatment in 1 atmosphere of hydrogen represents the irreversibly adsorbed fraction. The adsorption reversibility decreases markedly with increasing adsorption temperature as the surface species becomes more hydrogen deficient. The irreversibly adsorbed species have very long surface residence times on the order of days.

Figure 10: Hydrogen thermal desorption spectra illustrating the sequential dehydrogenation of ethylene, propylene, and cis-2-butene chemisorbed on Pt(111) at about 120 K (the heating rate is 12 K per second).

Figure 11: Surface Structure of Benzene as determined from low energy electron diffraction studies and surface crystallography.

Figure 12: The vibrational spectra of benzene and deuterated benzene as determined by high resolution electron energy loss spectroscopy.

Figure 13: Surface structures for alkylidyne species formed on platinum (111) after the adsorption and rearrangement of ethylene, propylene and butenes. These structures were determined by LEED surface crystallography.

Figure 14: The surface structure of ethylidyne, the bond distances and angles, are compared with several tri-nuclear metal cluster compounds of similar structure.

Figure 15: Changes of the vibrational spectrum of chemisorbed ethylene as a function of increasing temperature. Sequential decomposition is clearly visible from the vibrational spectrum obtained by high resolution electron energy loss spectroscopy.

Figure 16: Schematic representation of the various organic fragments that are present on metal surfaces at higher temperature. The presence of CH, C_2, C_2H, CH_2 and $C-CH_3$ species have been detected.

Figure 17: Fractional concentrations of uncovered platinum surface sites determined by CO adsorption desorption as a function of surface carbon coverage on the (100), (111), and (13,1,1) platinum crystal surfaces. A comparison is made between the CO uptake determined

Figure 17: (cont.) following n-hexane reaction studies and CO uptake determined when CO was coadsorbed with graphitic surface carbon.

Figure 18: Model for the working platinum catalyst that was developed from our combination of surface studies using single crystal surfaces and hydrocarbon reaction rate studies on these same surfaces.

Figure 19: Heat of desorption (kcal/mole) of CO and D_2 from lanthanum oxide, fresh and used lanthanum rhodate, fresh and used rhodium oxide and rhodium metal. The spread of each value represents the variation with surface coverage rather than experimental uncertainty.

Figure 20: A proposed mechanism for the photodissociation of water over TiO_2 and $SrTiO_3$ surfaces.

Figure 21: The rate of formation of various products from n-hexane as a function of fractional gold surface coverage for gold platinum alloys that were prepared by vaporizing and diffusing gold into Pt(111) crystal surfaces.

Figure 22: The heat of adsorption of potassium on platinum single crystal surfaces as a function of potassium coverage.

Figure 23: CO thermal desorption spectrum from clean platinum and when coadsorbed with potassium on platinum crystal surfaces.

Figure 24: Vibrational spectra of CO at the saturation coverage when chemisorbed on Pt(111) at 300 K as a function of preadsorbed potassium coverage.

Figure 25: Activation energy of the hydrogen β-elimination from carbonaceous deposits after n-hexane reactions over platinum (111) surfaces as a function of potassium coverages.

Figure 26 (a),(b) and (c): Standard free energies for several chemical reactions.

REFERENCES

1. F. Satterfield "Heterogeneous Catalysis in Practice", McGraw-Hill, New York (1980).

2. G.A. Somorjai, Chemistry in Two Dimensions: Surfaces, Cornell University Press, (1981). Library of Congress Catalog Card No. 80-21443.

3. "Heterogeneous Catalysis", ed. B. Davis and W. Hettinger, ACS Monograph 222 (1983).

4. G.A. Somorjai, Proc. of Welch Conf. 25 (1981) 83.

5. A.L. Cabrera, N.D. Spencer, E. Kozak, P.W. Davies and G.A. Somorjai, Rev. Sci. Instru. 53(12) (1982) 1888.

6. G. Ertl, Proc. of Welch Conf. 25 (1981) 179.

7. M. Asscher, W.L. Guthrie, T.-H. Lin and G.A. Somorjai, J. Chem. Phys. 78(11) (1983) 6992.

8. D.R. Kahn, E.E. Petersen and G.A. Somorjai, J. Catal. 34 (1974) 294.

9. S.M. Davis and G.A. Somorjai, J. Catal. 65 (1980) 78.

10. B.A. Sexton and G.A. Somorjai, J. Catal. 46 (1977) 167.

11. N.D. Spencer, R.C. Schoonmaker and G.A. Somorjai, J. Catal. 74 (1982) 129.

12. L. Falicov and G.A. Somorjai, Proc. Natl. Acad. of Sci., to be published (1984).

13. M. Asscher and G.A. Somorjai, Surf. Sci., in press (1984).

14. D.W. Blakely and G.A. Somorjai, Surf. Sci. 65 (1977) 419.

15. R.W. Joyner and G.A. Somorjai, The Chem. Soc. Publ. 2 (1973) 1.

16. B. Lang, R.W. Joyner and G.A. Somorjai, Surf. Sci. 30 (1972) 454.

17. M. Salmeron, R.J. Gale and G.A. Somorjai, J. Chem. Phys. 67 (1977) 5324.

18. W.D. Gillespie, R.K. Herz, E.E. Petersen and G.A. Somorjai, J. Catal. 70 (1981) 147.

19. S.M. Davis, F. Zaera and G.A. Somorjai, J. Catal. 85(1) (1984) 206.

20. S.M. Davis, F. Zaera and G.A. Somorjai, J. Am. Chem. Soc. 104 (1982) 7453.

21. R.K. Herz, W.D. Gillespie, E.E. Petersen and G.A. Somorjai, J. Catal. 67 (1981) 371.

22. S.M. Davis, F. Zaera and G.A. Somorjai, J. Catal. 77 (1982) 439.

23. S.M. Davis, B.E. Gordon, M. Press and G.A. Somorjai, J. Vac. Sci. & Techn. 19 (1981) 231.

24. M. Salmeron and G.A. Somorjai, J. Phys. Chem. 86 (1982) 341.

25. R.J. Koestner, M.A. Van Hove and G.A. Somorjai, J. Phys. Chem. 87 (1983) 203.

26. M.A. Van Hove, R. Lin and G.A. Somorjai, Phys. Rev. Lett. 51(9) (1983) 778.

27. B.E. Koel, J.E. Crowell, C.M. Mate and G.A. Somorjai, J. Phys. Chem., in press (1984).

28. R.J. Koestner, J.C. Frost, P.C. Stair, M.A. Van Hove and G.A. Somorjai, Surf. Sci. 116 (1982) 85.

29. R.J. Koestner, M.A. Van Hove and G.A. Somorjai, Surf. Sci. 121 (1982) 321.

30. G.A. Somorjai, Proc. 9th Intl. Conf. on Atomic Spectroscopy, XXII CSI, Tokyo, June 1982, Recent Advances in Analytical Spectroscopy, ed. K. Fuwa, Pub. Pergamon Press, (1982) 211.

31. B.E. Koel, J.E. Crowell, C.M. Mate and G.A. Somorjai, J. Phys. Chem., submitted for publication (1984).

32. C. Minot, M.A. Van Hove and G.A. Somorjai, Surf. Sci. 127 (1982) 441.

33. F. Zaera and G.A. Somorjai, J. Am. Chem. Soc., in press (1983).

34. S.M. Davis, W.D. Gillespie and G.A. Somorjai, J. Catal. 83 (1983) 131.

35. D.G. Castner, R.L. Blackadar and G.A. Somorjai, J. Catal. 66 (1980) 257.

36. P.R. Watson and G.A. Somorjai, J. Catal. 74 (1982) 282.

37. F.T. Wagner, S. Ferrer and G.A. Somorjai, in Photoeffects at Semiconductor-Electrolyte Interfaces, ed. A.J. Nozik, ACS Symposium Series 146, Washington, (1981).

38. F.T. Wagner and G.A. Somorjai, J. Am. Chem. Soc. 102 (1980) 5494.

39. Van Damme and K. Hall, J. Am. Chem. Soc. 101 (1980) 4373.

40. J.W.A. Sachtler, M.A. Van Hove, J.P. Biberian and G.A. Somorjai, Surf. Sci. 110 (1981) 19.

41. J.W.A. Sachtler and G.A. Somorjai, J. Catal. 81 (1983) 77.

42. Y-L. Lam, J. Criado and M. Boudart, Nouveau J. de Chimie I (1977) 461.

43. E.L. Garfunkel and G.A. Somorjai, Surf. Sci. 115 (1982) 441.

44. E.L. Garfunkel, J.E. Crowell and G.A. Somorjai, J. Phys. Chem. 86 (1982) 310.

45. J.E. Crowell, E.L. Garfunkel and G.A. Somorjai, Surf. Sci. 121 (1982) 303.

46. F. Zaera and G.A. Somorjai, J. Catal. 84(2) (1983) 375.

47. E.L. Garfunkel, J.J. Maj, J.C. Frost, M.H. Farias and G.A. Somorjai, J. Phys. Chem. 87(19) (1983) 3629.

48. R. Casanova, A.L. Cabrera, H. Heinemann and G.A. Somorjai, Fuel 62 (1983)1138.

49. F. Delannay, W.T. Tysoe, H. Heinemann and G.A. Somorjai, Carbon, in press (1984).

50. M.M. Khan and G.A. Somorjai, J. Catal., submitted for publication (1984).

51. C. Leygraf, M. Hendewerk and G.A. Somorjai, J. Catal. 78 (1982) 341.

52. H.W.K. Tom, C.M. Mate, X.D. Zhu, J.E. Crowell, T.F. Heinz, Y.R. Shen and G.A. Somorjai, Phys. Rev. Letters, in press (1984).

TABLE I

Table of surface characterization techniques that are used to determine the structure and composition of solid surfaces. Adsorbed species present at concentrations of 1% of a monolayer can be readily detected.

SURFACE ANALYSIS METHOD	ACRONYM	PHYSICAL BASIS	TYPE OF INFORMATION OBTAINED
Low energy electron diffraction	LEED	Elastic backscattering low energy electrons	Atomic surface structure of surfaces and of adsorbed gases
Auger electron spectroscopy	AES	Electron emission from surface atoms excited by electron x-ray or ion bombardment	Surface composition
High resolution electron energy loss spectroscopy	HREELS	Vibrational excitation of surface atoms by inelastic reflection of low energy electrons	Structure and bonding of surface atoms and adsorbed species.
Infrared spectroscopy	IRS	Vibrational excitation of surface atoms by adsorption of infrared radiation.	Structure and bonding of adsorbed gases.
X-ray and ultraviolet photoelectron spectroscopy	XPS UPS	Electron emission from atoms	Electronic structure and oxidation state of surface atoms and adsorbed species.
Ion scattering spectroscopy	ISS	Inelastic reflection of inert gas ions.	Atomic structure and composition of solid surfaces
Secondary ion mass spectroscopy	SIMS	Ion beam induced ejection of surface atoms as positive & negative ions	Surface composition
Extended X-ray absorption fine structure analysis	EXAFS	Interference effects during x-ray emission	Atomic structure energetics composition of adsorbed species
Thermal desorption spectroscopy	TDS	Thermally induced desorption or decomposition of adsorbed species	Adsorption energetics composition of adsorbed species
Solid state nuclear magnetic resonance	Solid-state NMR	Nuclear magnetic resonance on samples with areas of 1 m^2 or larger	Atomic and molecular composition, structure

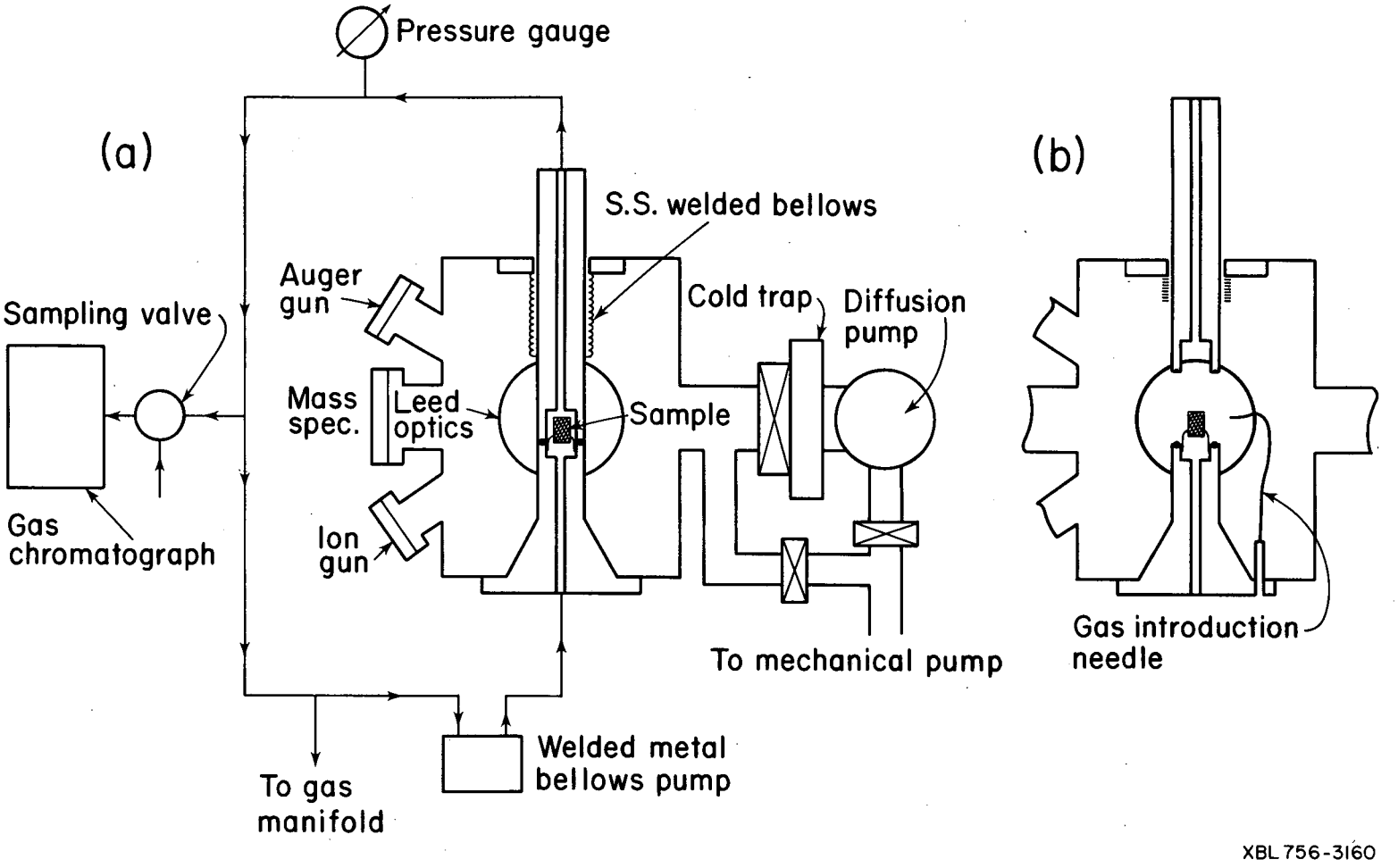
Pressure gauge
(a)
(b)
S.S. welded bellows
Auger gun
Sampling valve
Cold trap
Diffusion pump
Mass spec.
Leed optics
Sample
Gas chromatograph
Ion gun
To mechanical pump
Gas introduction needle
Welded metal bellows pump
To gas manifold
XBL 756-3160

Fig. 1

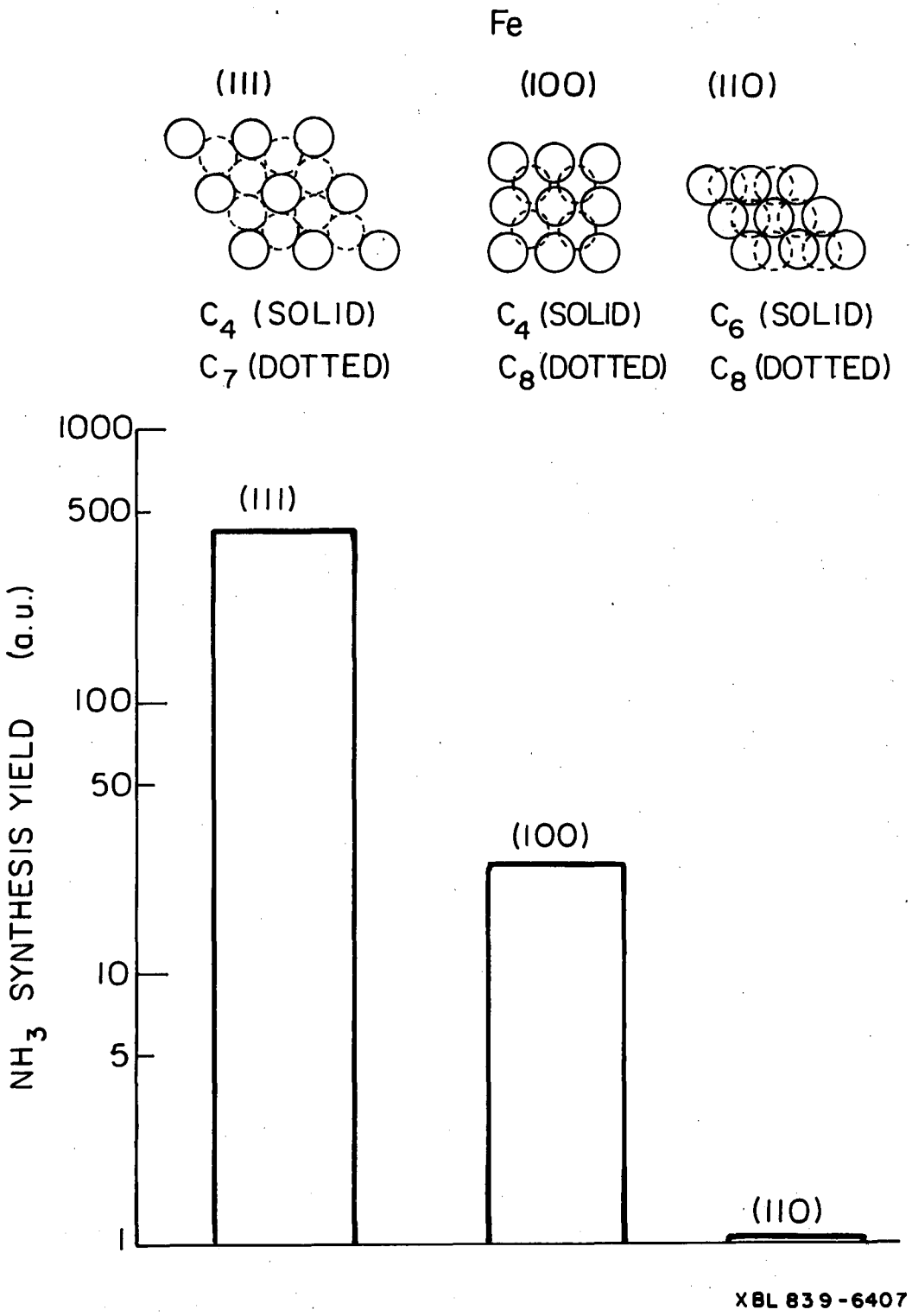
Fe
(111)
(100)
(110)
C4 (SOLID)
C7 (DOTTED)
C4 (SOLID)
C8 (DOTTED)
C6 (SOLID)
C8 (DOTTED)
1000
500
100
50
10
5
1
NH3 SYNTHESIS YIELD (a.u.)
(111)
(100)
(110)
XBL 839-6407

Fig. 2

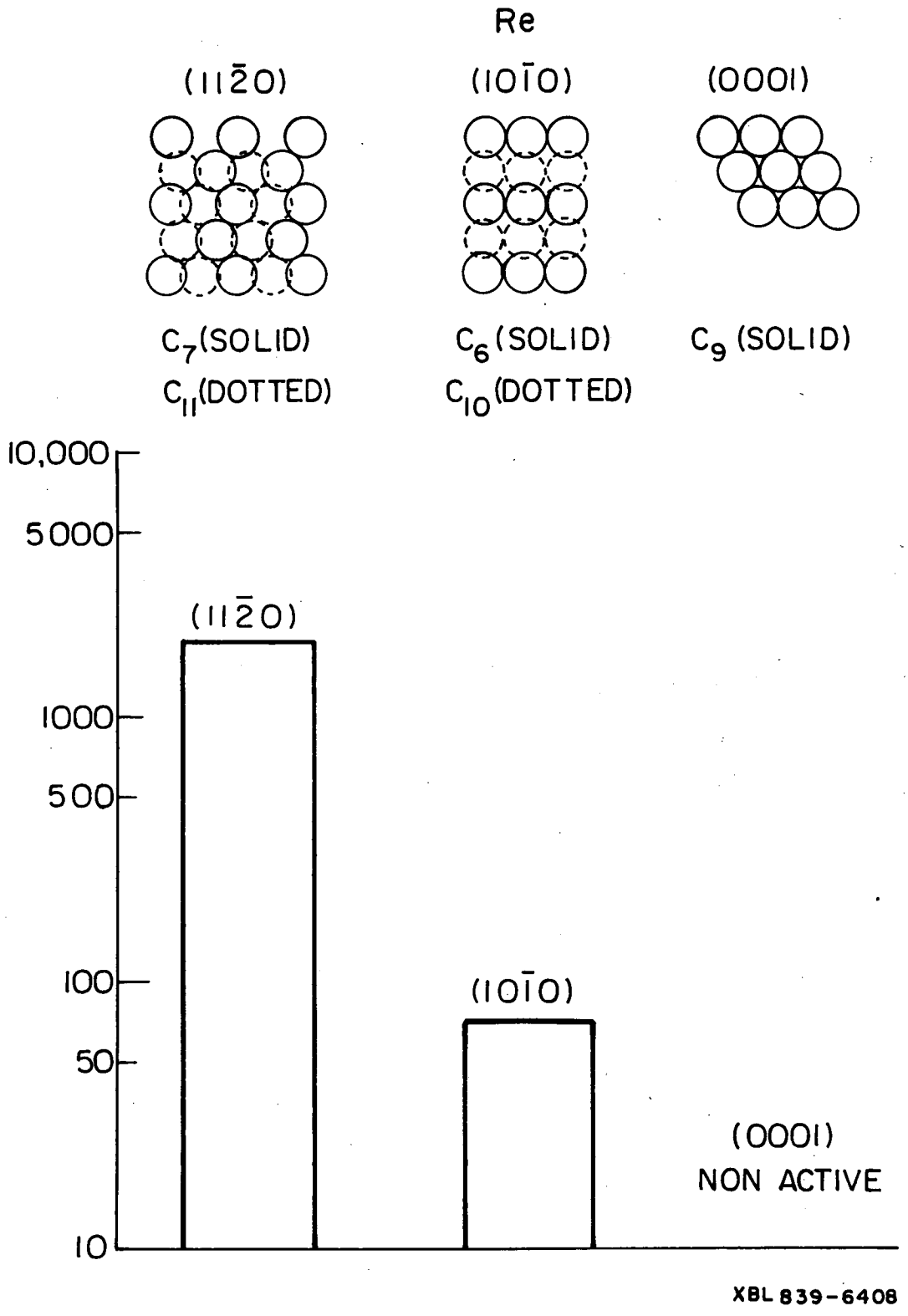
Re
(11$\bar{2}$0)
(10$\bar{1}$0)
(0001)
C_7(SOLID)
C_{11}(DOTTED)
C_6(SOLID)
C_{10}(DOTTED)
C_9 (SOLID)
10,000
5000
1000
500
100
50
10
(11$\bar{2}$0)
(10$\bar{1}$0)
(0001)
NON ACTIVE
XBL 839-6408

Fig. 3

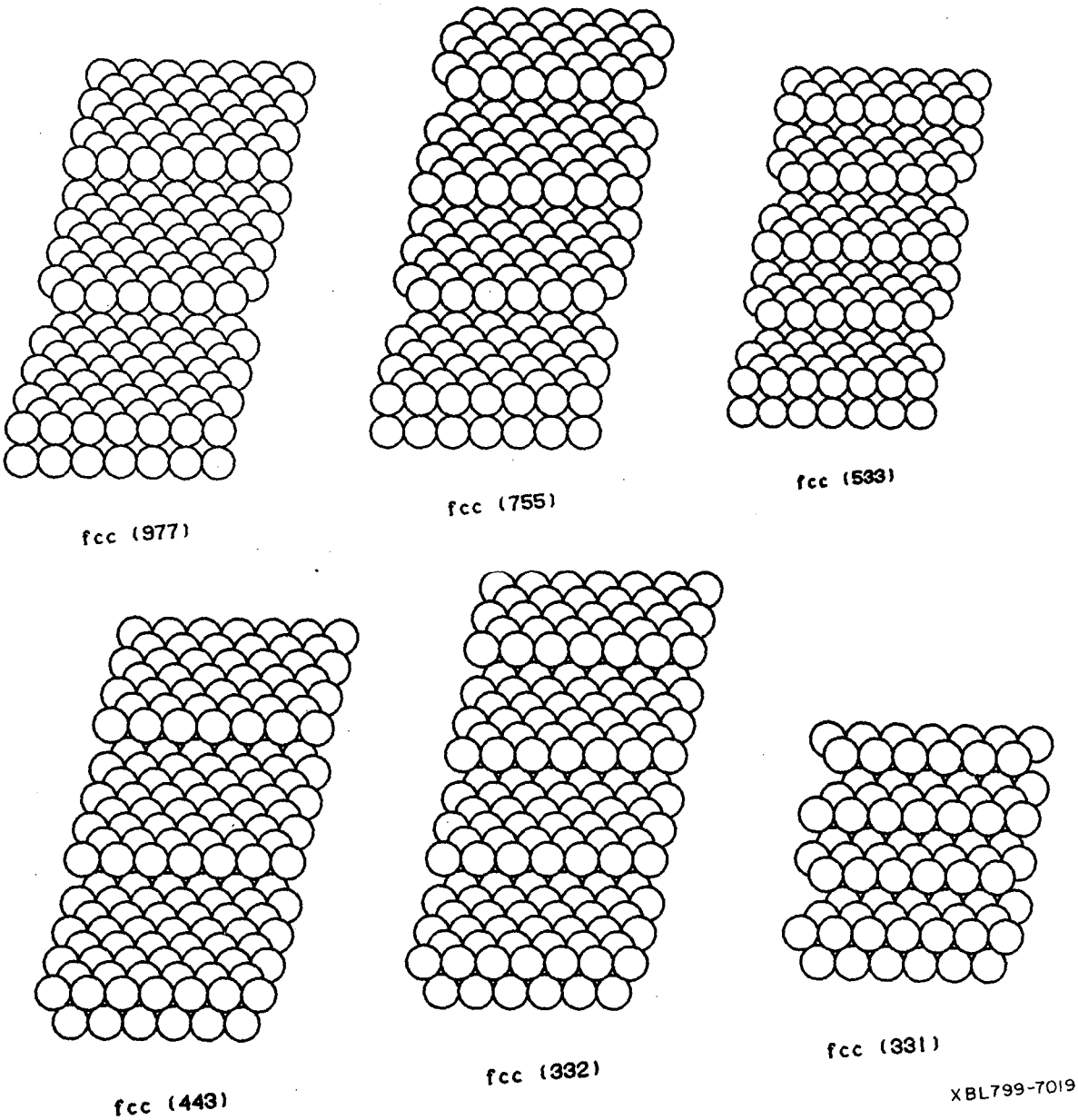

Fig. 4

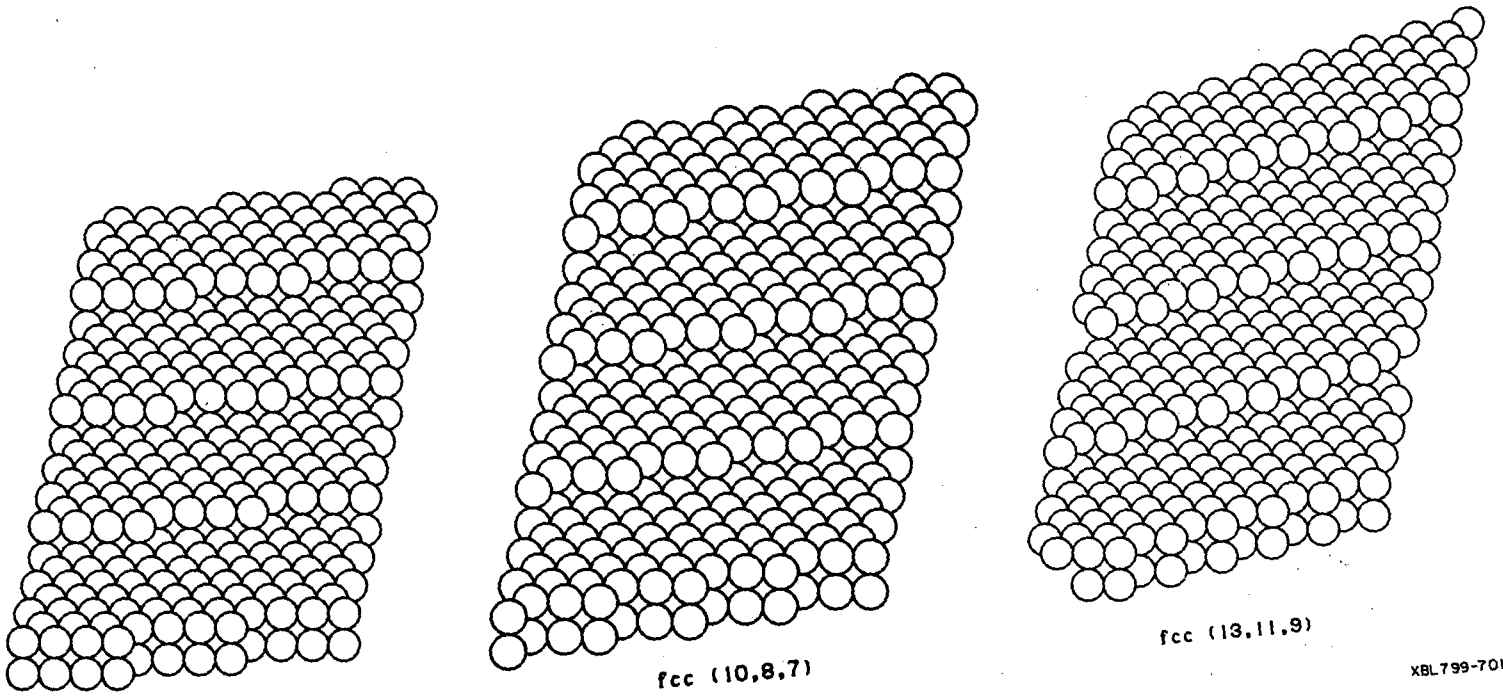

Fig. 5

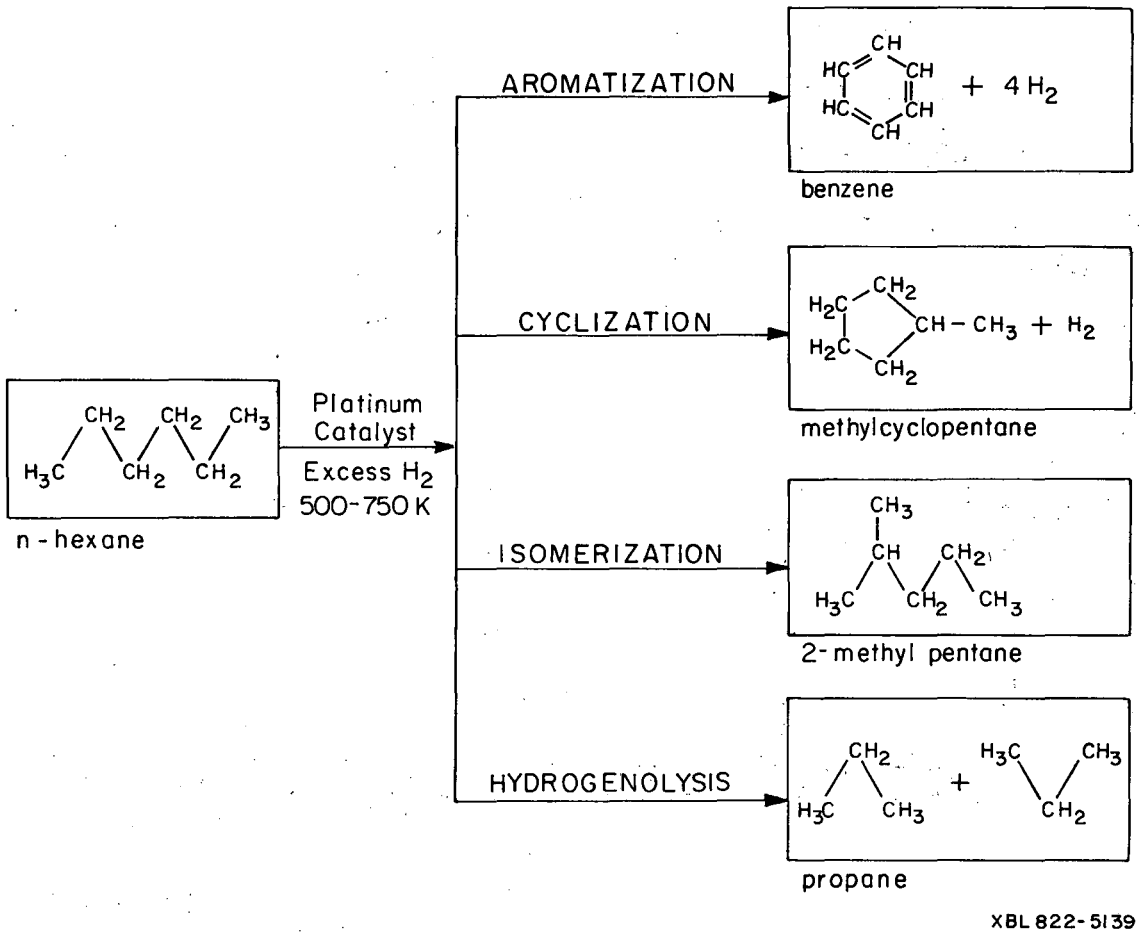
n - hexane
Platinum Catalyst
Excess H_2
500-750 K
AROMATIZATION
benzene
+ 4 H_2
CYCLIZATION
methylcyclopentane
+ H_2
ISOMERIZATION
2-methyl pentane
HYDROGENOLYSIS
propane
XBL 822-5139

Fig. 6

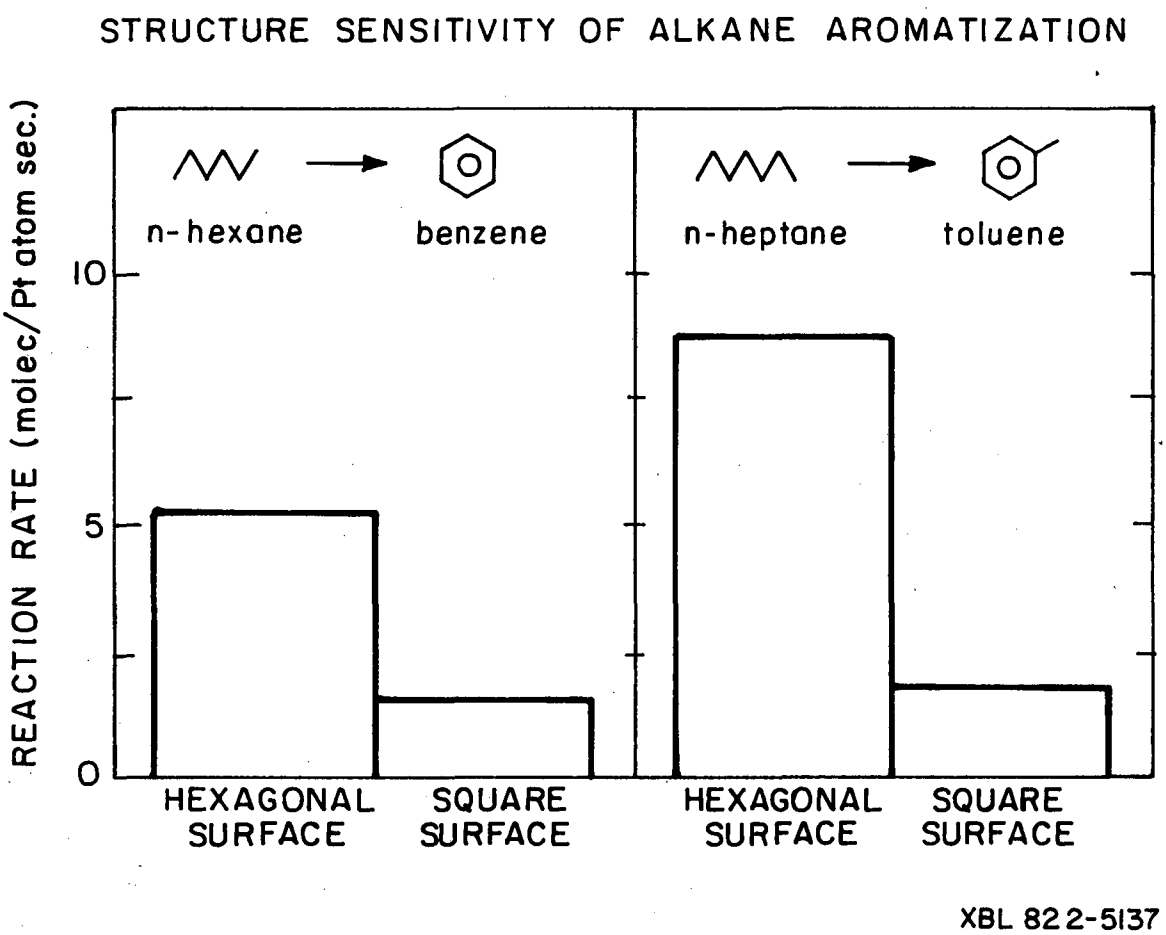
STRUCTURE SENSITIVITY OF ALKANE AROMATIZATION
REACTION RATE (molec/Pt atom sec.)
10
5
0
n-hexane
benzene
n-heptane
toluene
HEXAGONAL SURFACE
SQUARE SURFACE
HEXAGONAL SURFACE
SQUARE SURFACE
XBL 822-5137

Fig. 7

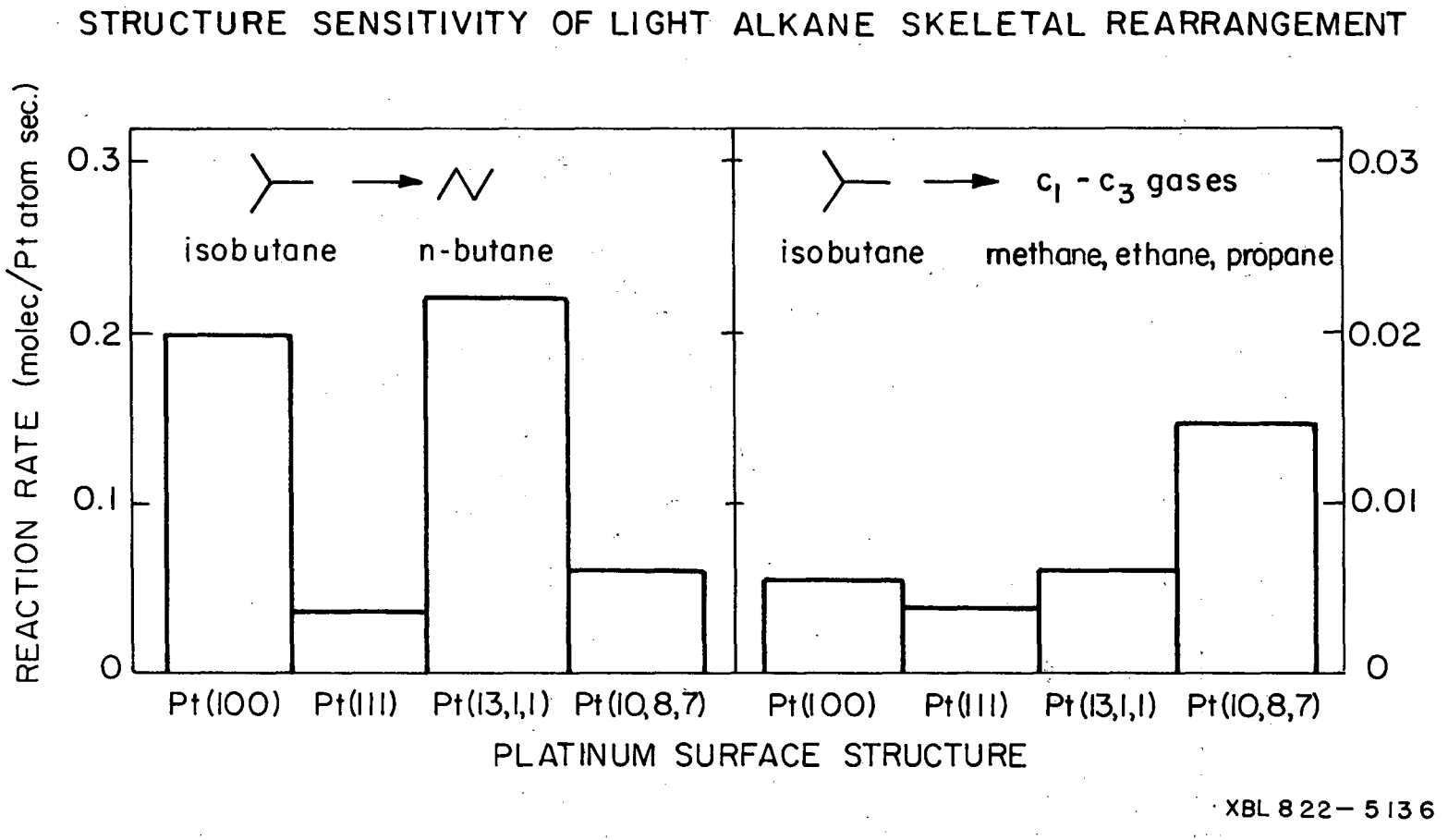

XBL 822-5136

Fig. 8

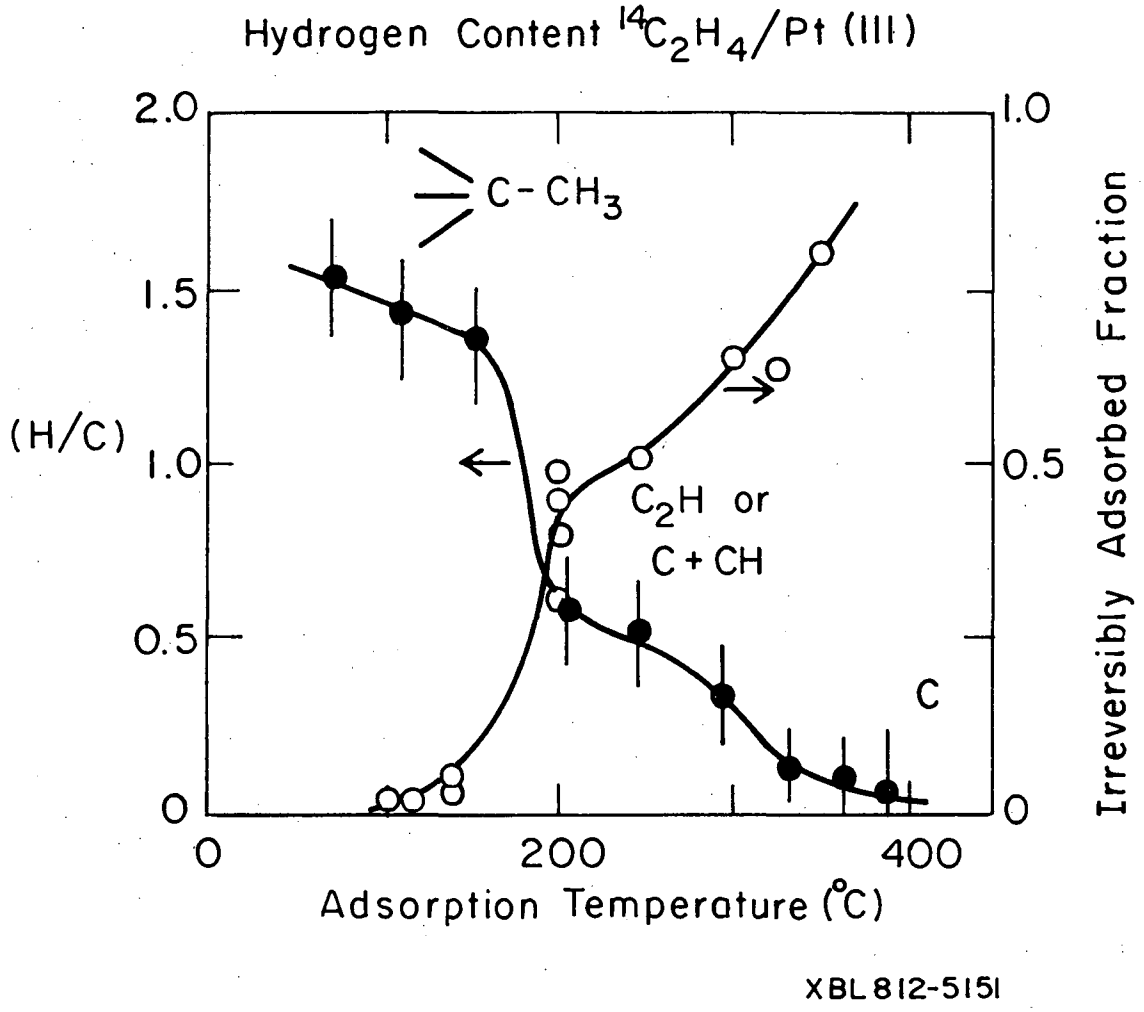
Hydrogen Content $^{14}C_2H_4$/Pt (III)
2.0
1.5
1.0
0.5
0
(H/C)
1.0
0.5
0
Irreversibly Adsorbed Fraction
C-CH3
C2H or
C + CH
C
0
200
400
Adsorption Temperature (°C)
XBL 812-5151

Fig. 9

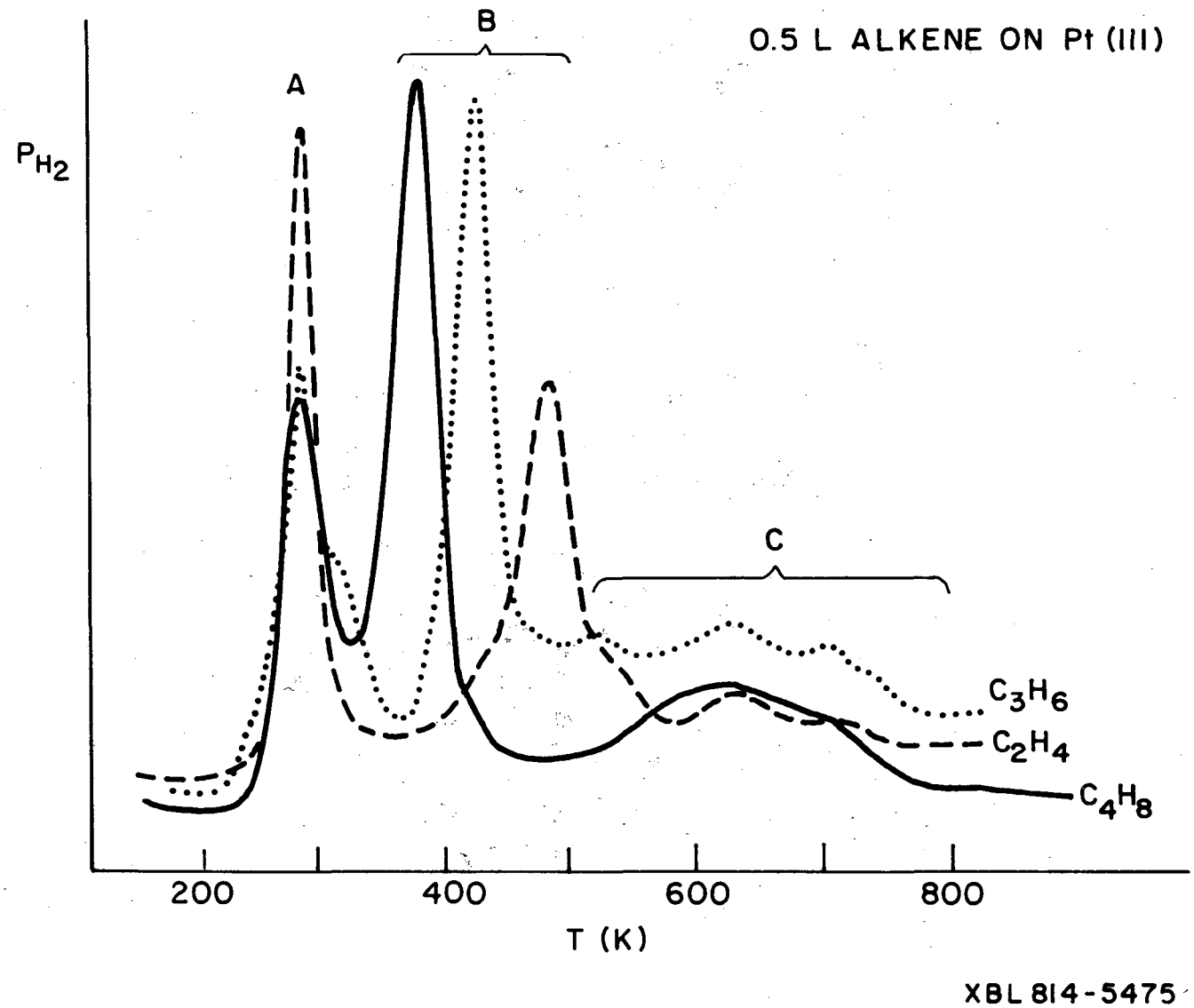
0.5 L ALKENE ON Pt (111)
A
B
C
P_{H_2}
C_3H_6
C_2H_4
C_4H_8
200
400
600
800
T (K)
XBL 814-5475

Fig. 10

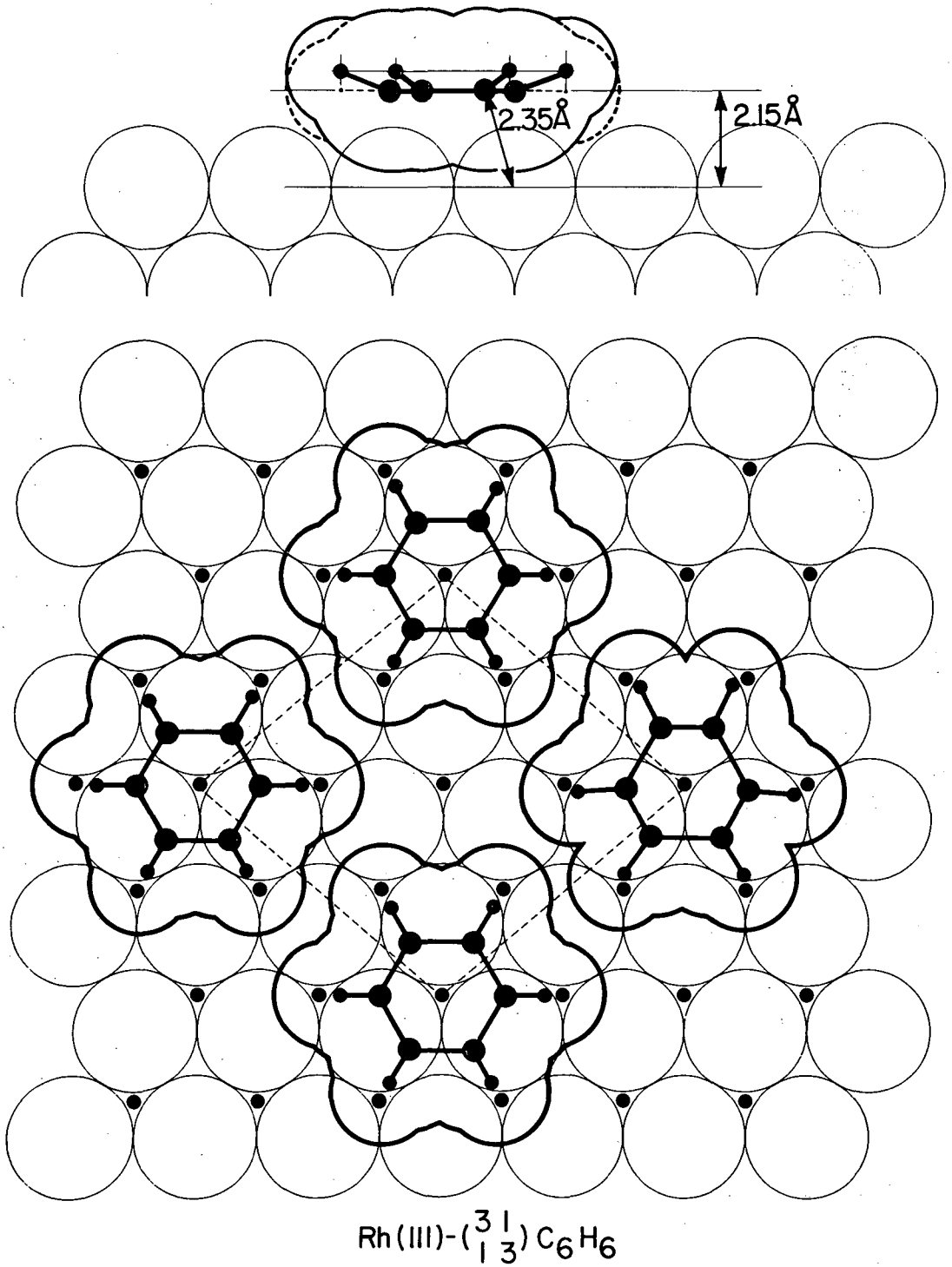

XBL 835-198

Fig. 11

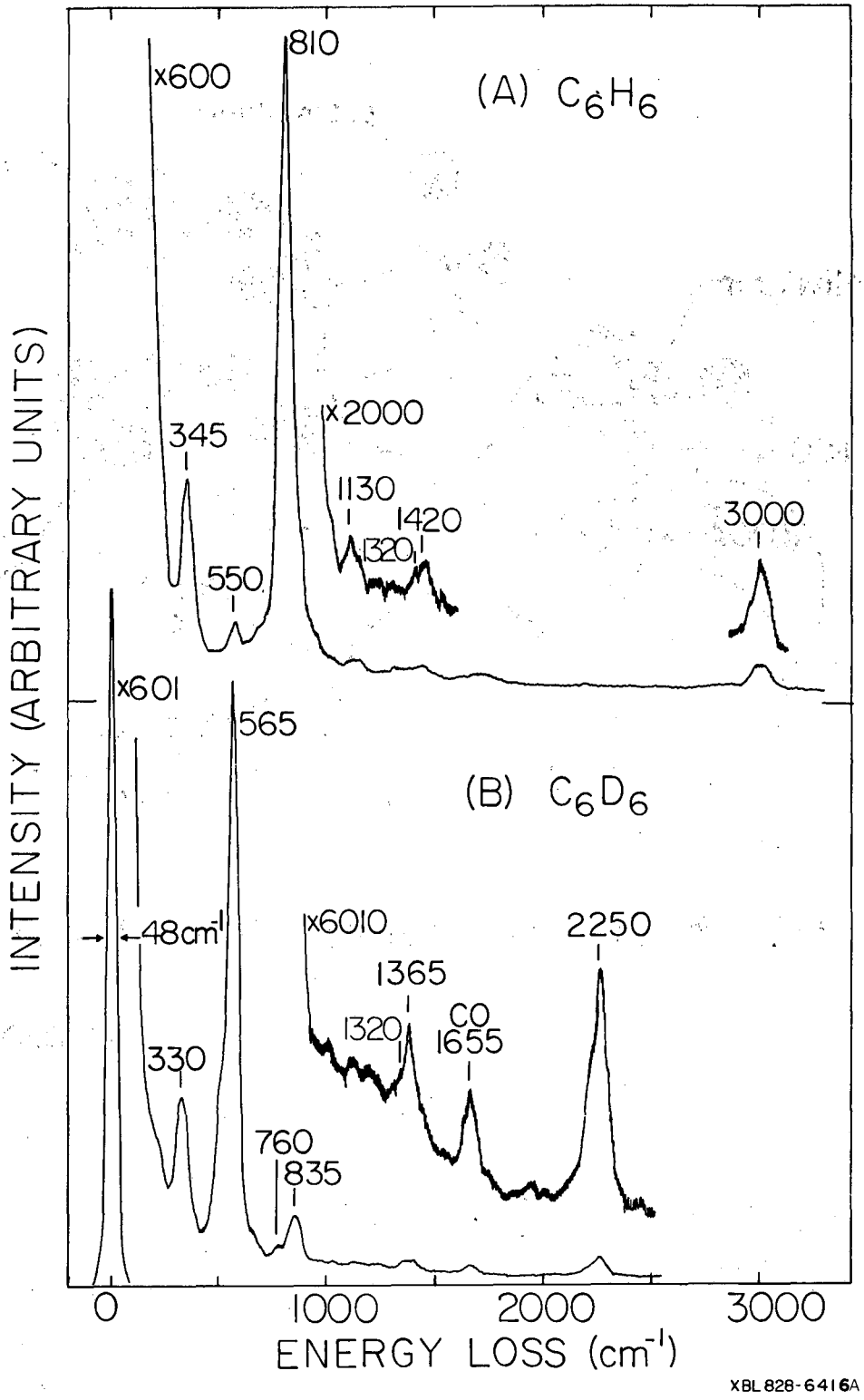
(A) C_6H_6
x600
810
345
550
x2000
1130
1320
1420
3000
(B) C_6D_6
x601
565
48cm⁻¹
x6010
1365
1320
CO
1655
2250
330
760
835
INTENSITY (ARBITRARY UNITS)
0
1000
2000
3000
ENERGY LOSS (cm⁻¹)
XBL 828-6416A

Fig. 12

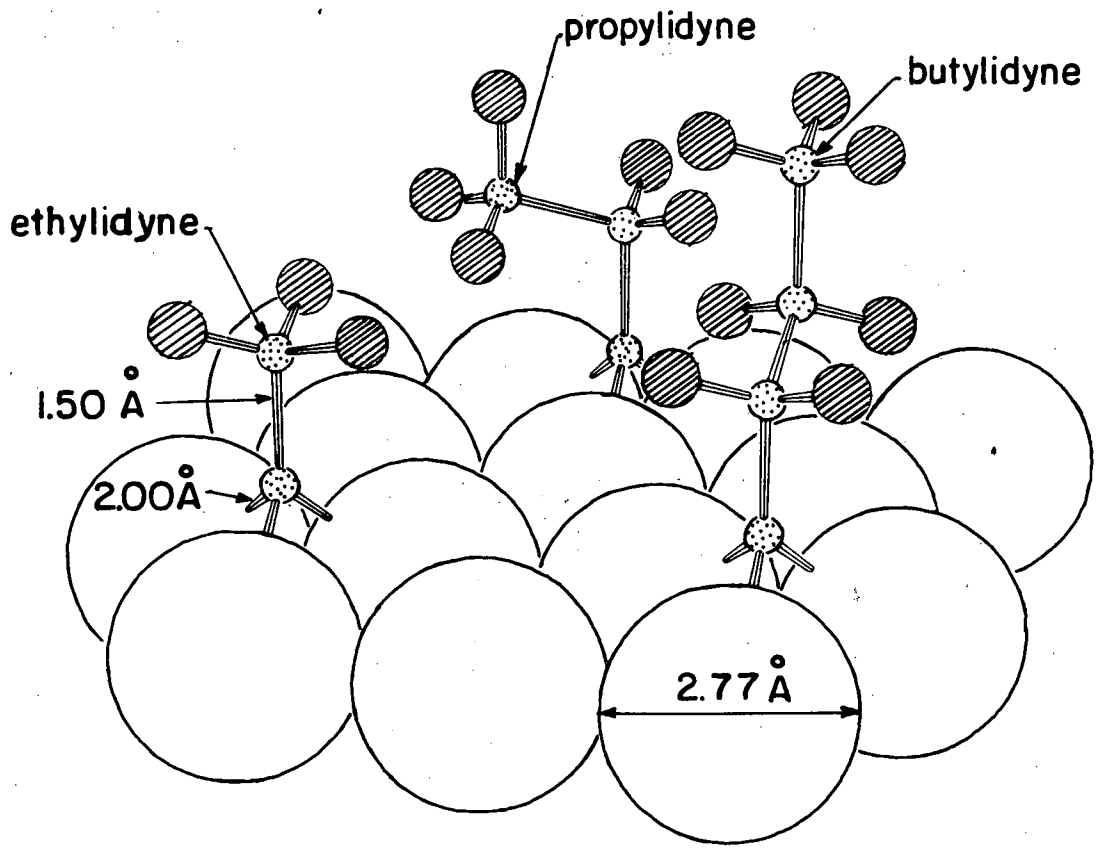

Pt (111) + ethylidyne, propylidyne and butylidyne

XBL 8110-6882

Fig. 13

Different ethylidyne species: bond distances and angles
(r_C = carbon covalent radius; r_M = bulk metal atomic radius)

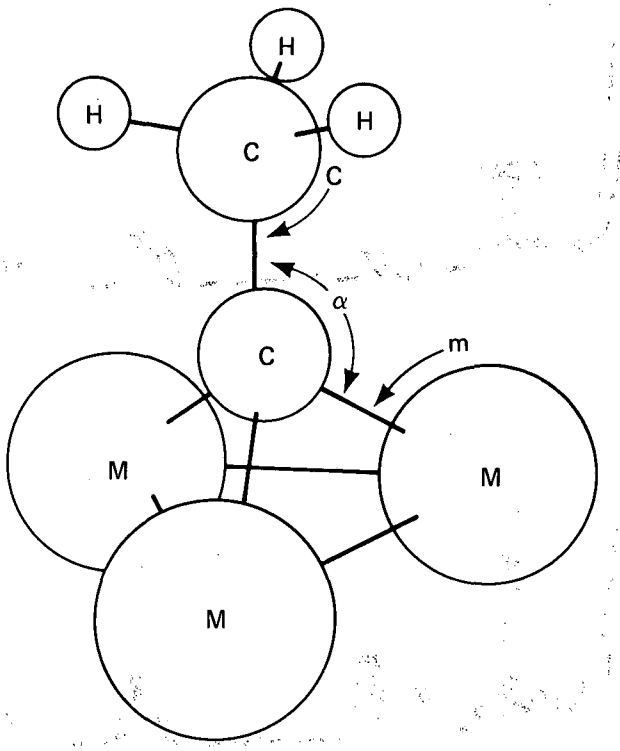

	C [Å]	m	r_M	r_C	α [°]
$Co_3(CO)_9CCH_3$	1.53 (3)	1.90 (2)	1.25	0.65	131.3
$H_3Ru_3(CO)_9CCH_3$	1.51 (2)	2.08 (1)	1.34	0.74	128.1
$H_3Os_3(CO)_9CCH_3$	1.51 (2)	2.08 (1)	1.35	0.73	128.1
Pt (111) + (2 X 2) CCH_3	1.50	2.00	1.39	0.61	127.0
Rh (111) + (2 X 2) CCH_3	1.45 (10)	2.03 (7)	1.34	0.69	130.2
H_3C-CH_3	1.54			0.77	109.5
$H_2C=CH_2$	1.33			0.68	122.3
$HC\equiv CH$	1.20			0.60	180.0

XBL 818-11196

Fig. 14

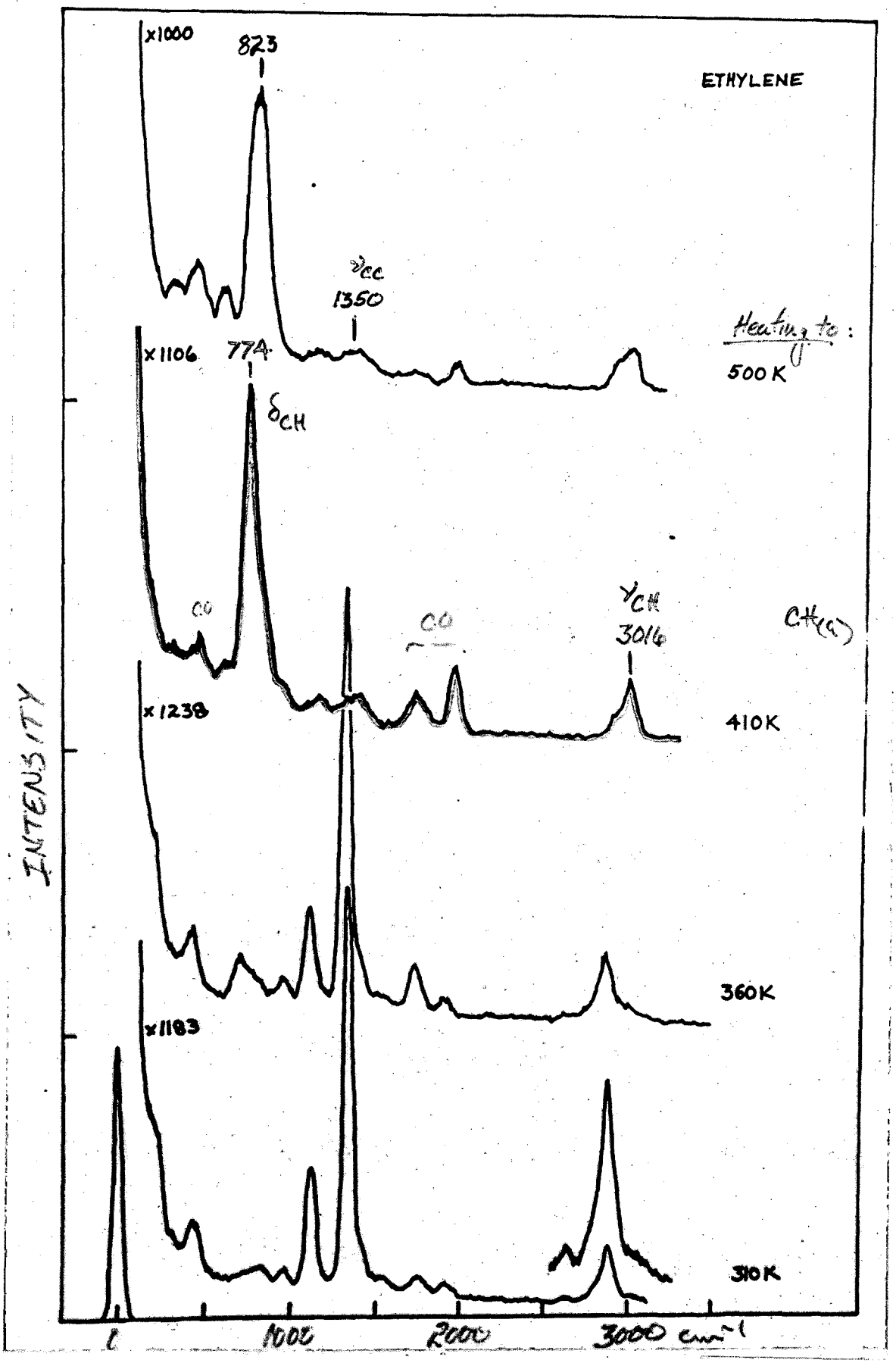

Fig. 15 CBB 834-2838

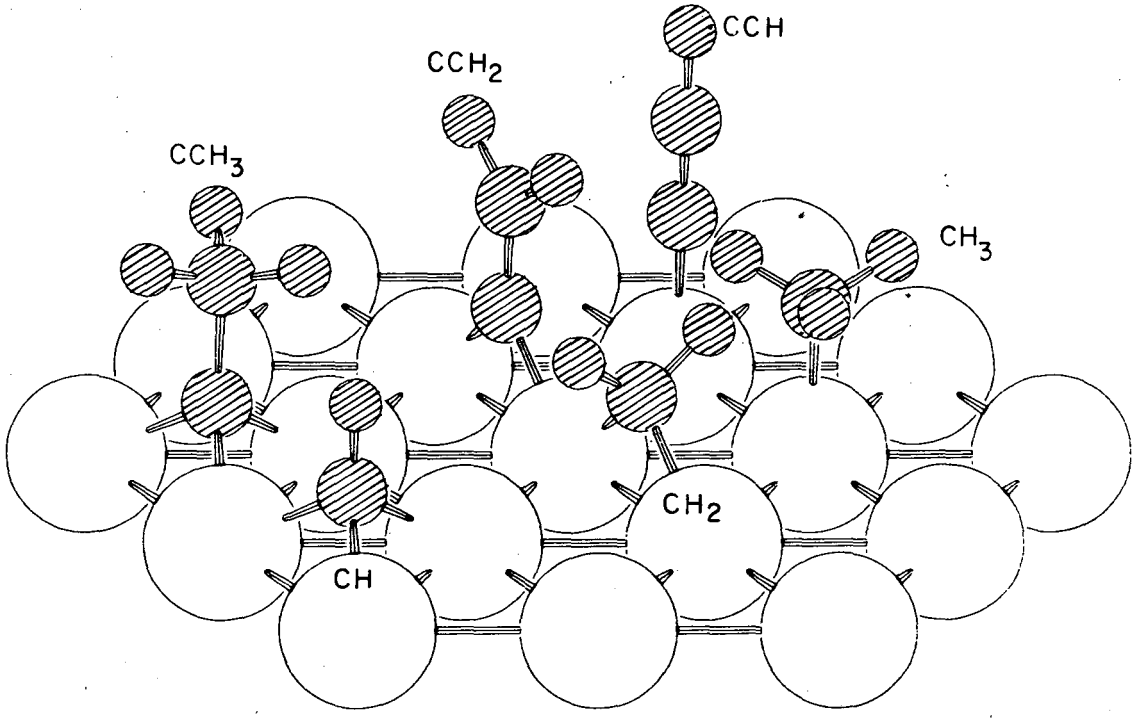

XBL 826-5941

Fig. 16

CO Chemisorption on Carbon Covered Pt(111), Pt(100) and Pt(13, 1,1)

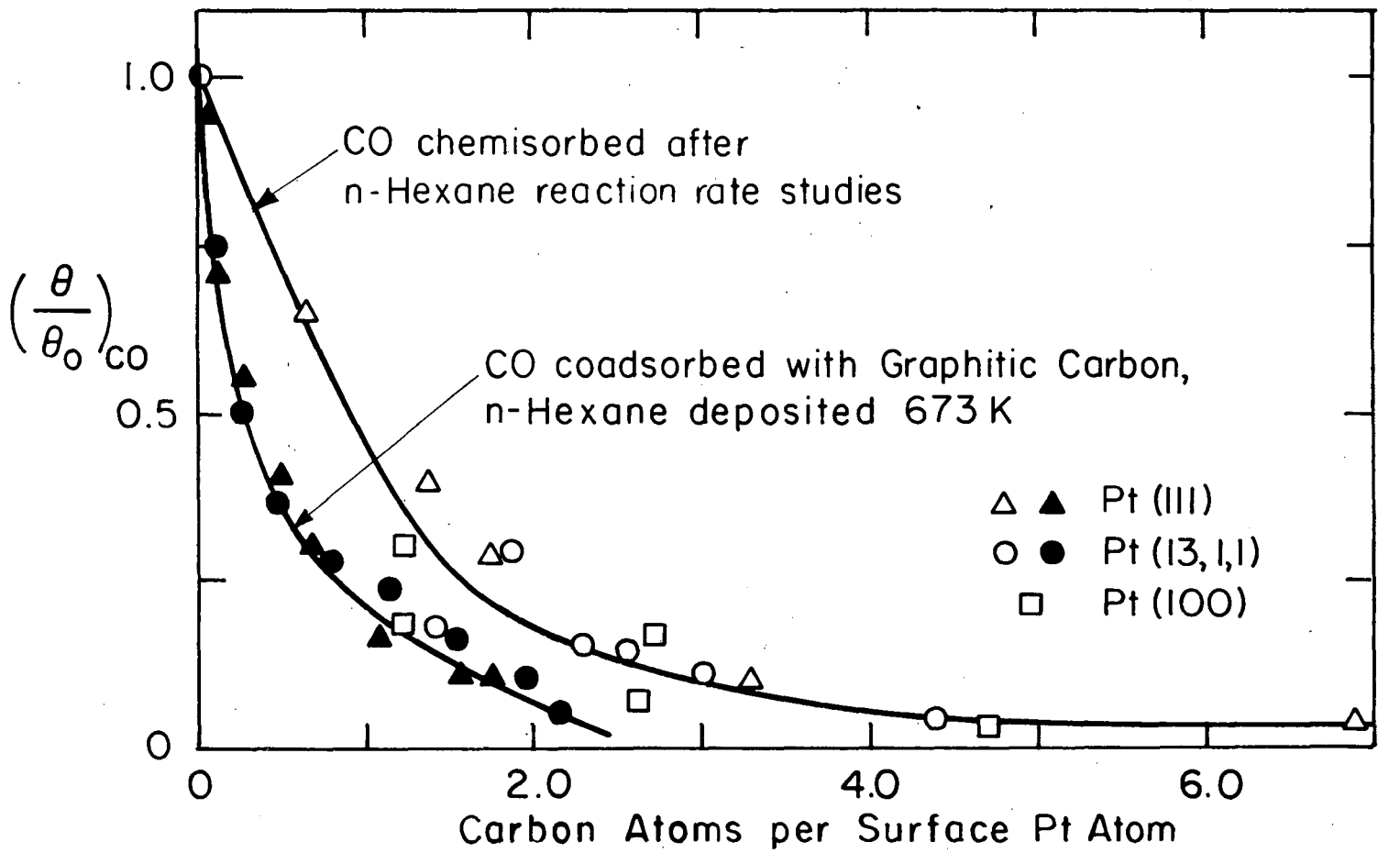

XBL 816-5851

Fig. 17

MODEL FOR THE WORKING PLATINUM CATALYST

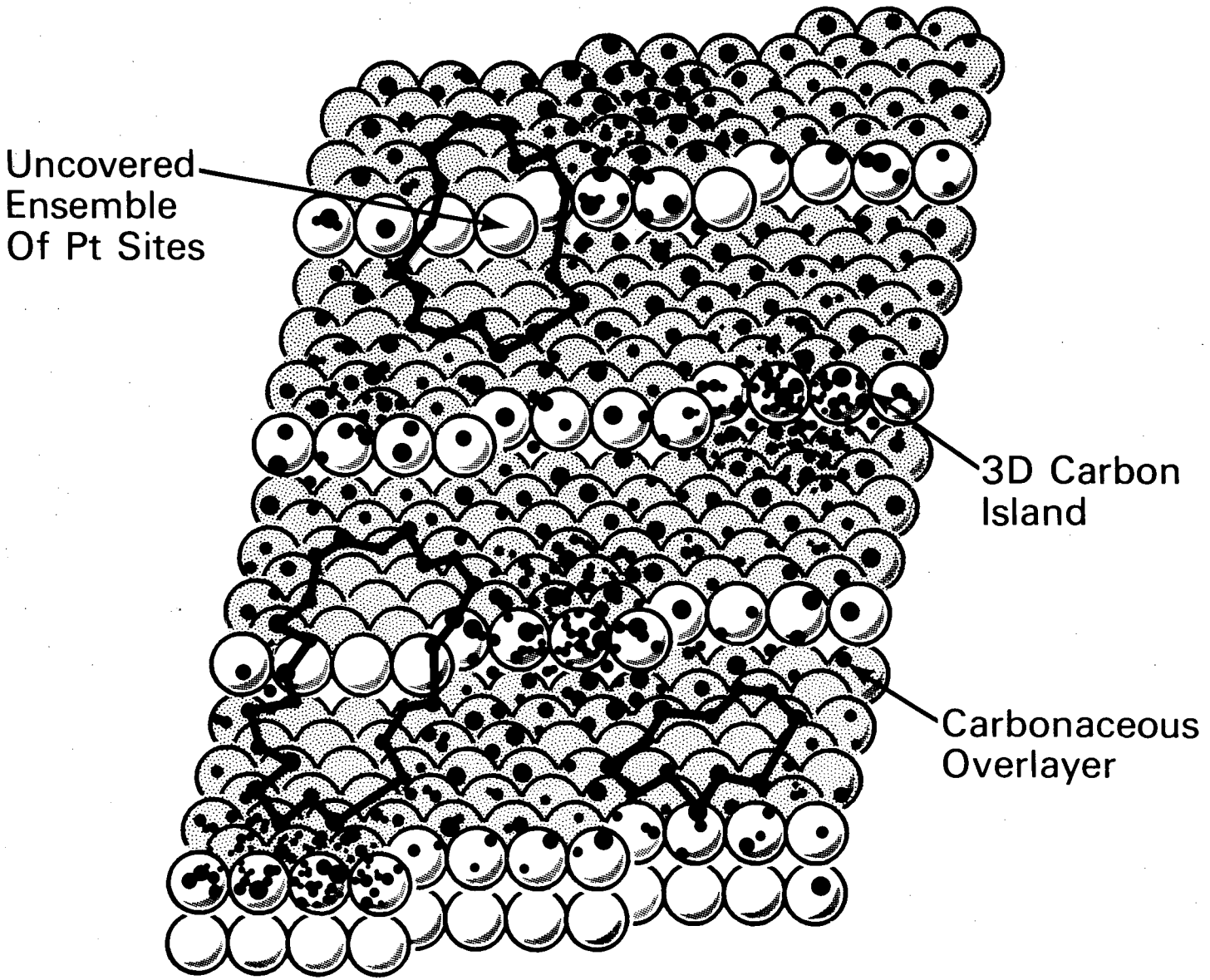

Fig. 18

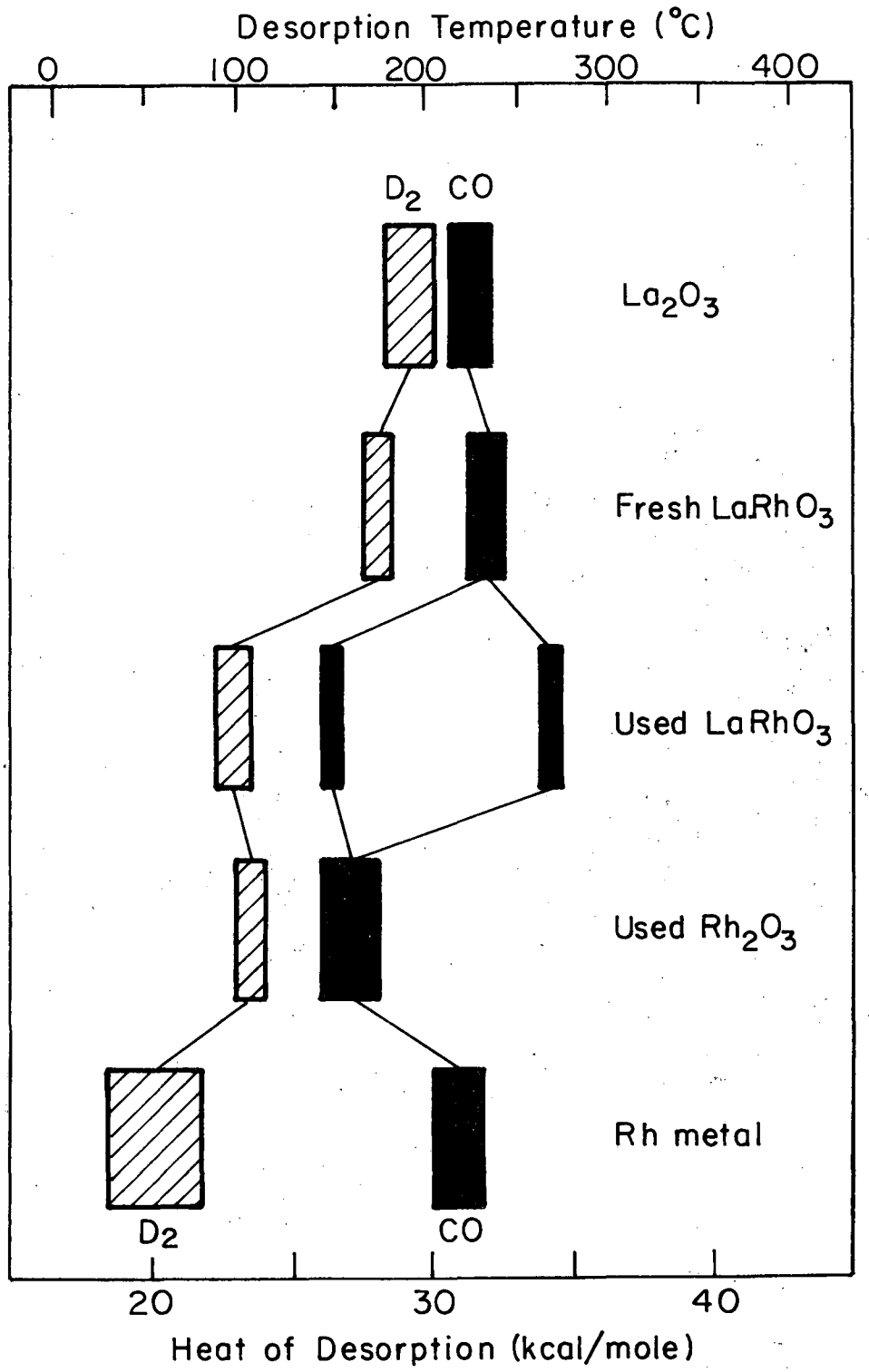

XBL 817-6123

Fig. 19

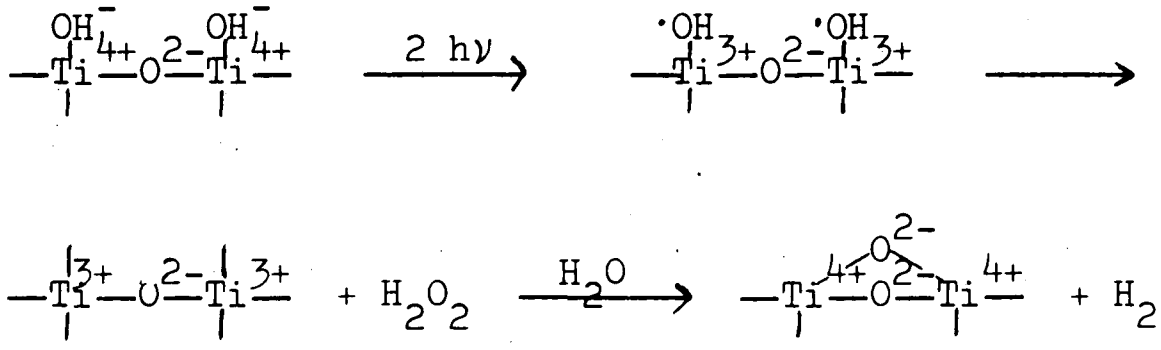

Van Damme and Hall, JACS 101 4373

XBL 822-7816

Fig. 20

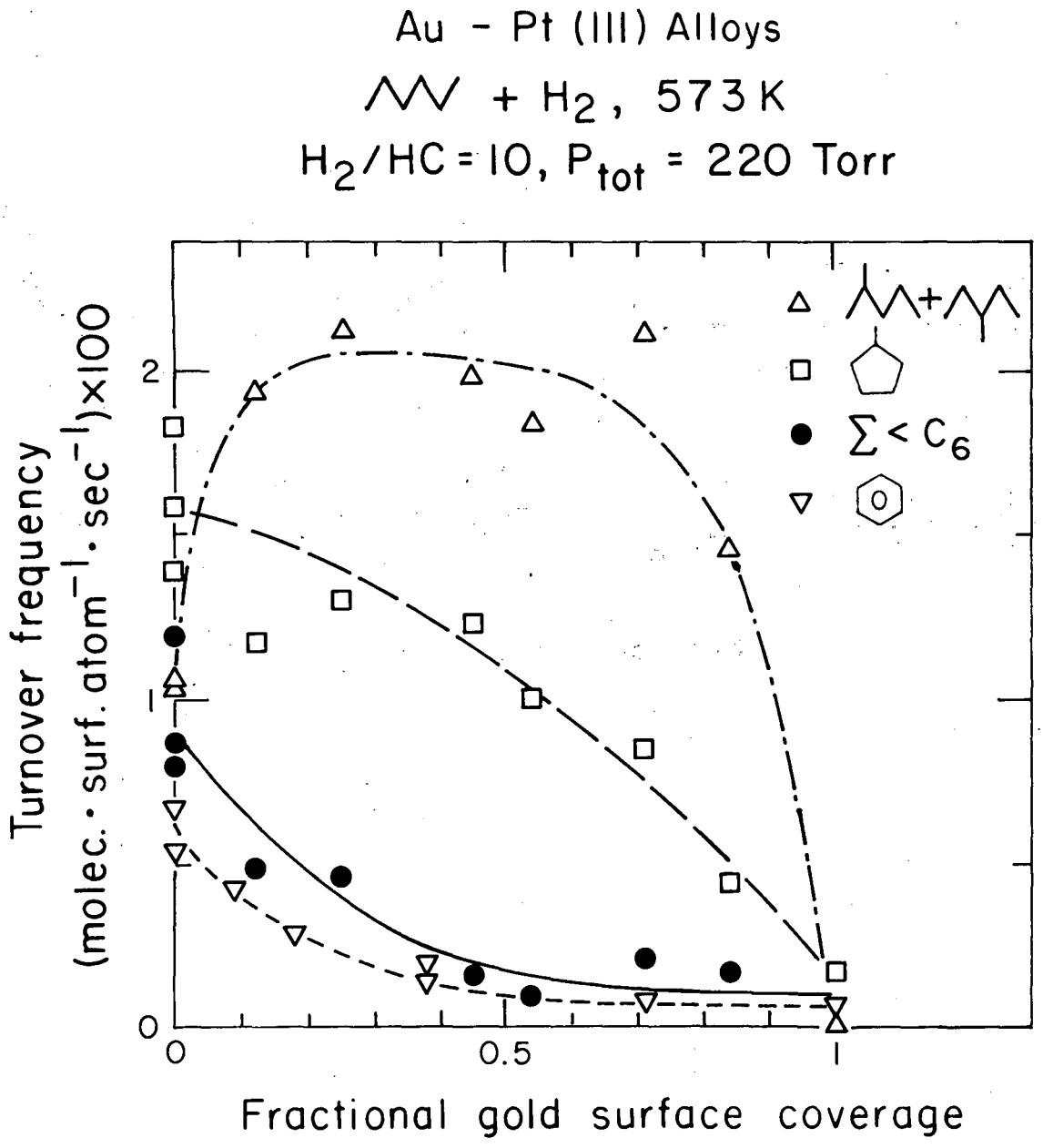

XBL 819-2495

Fig. 21

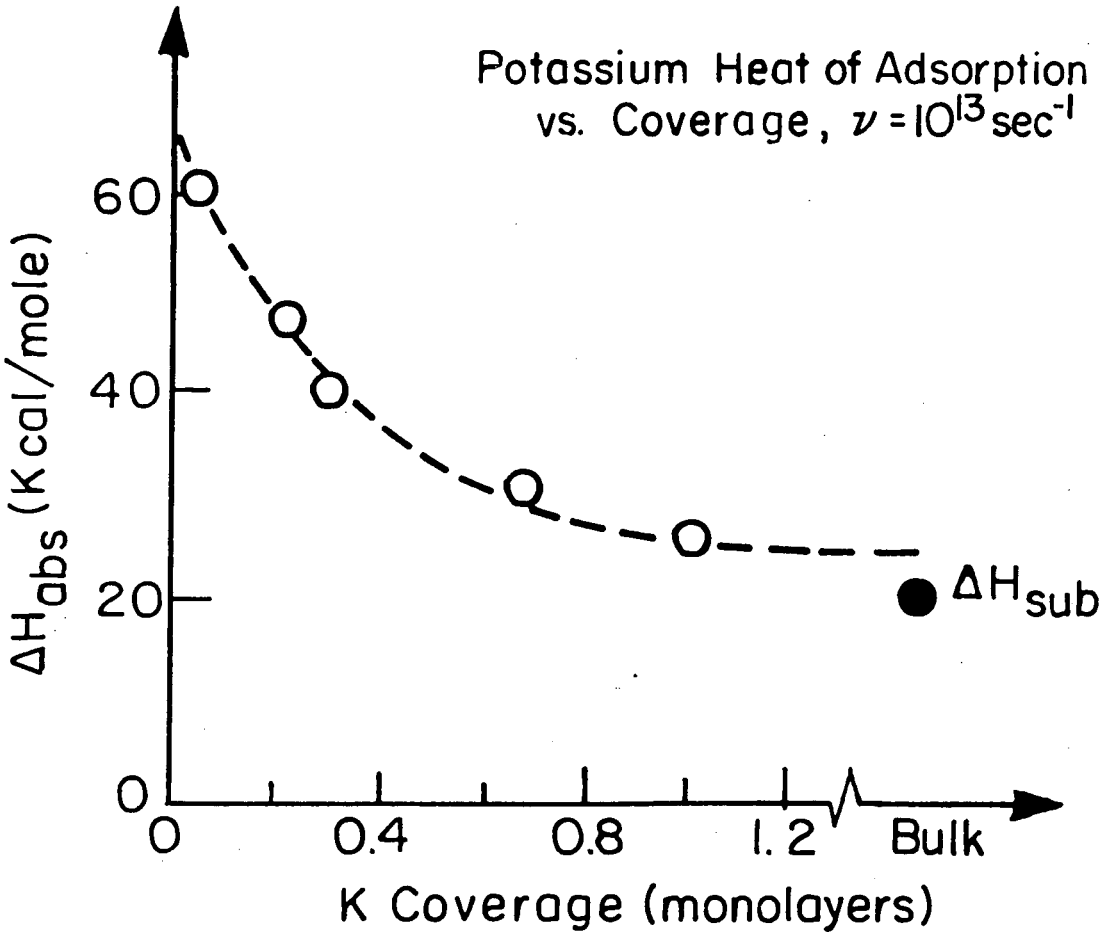

XBL816-5910B

Fig. 22

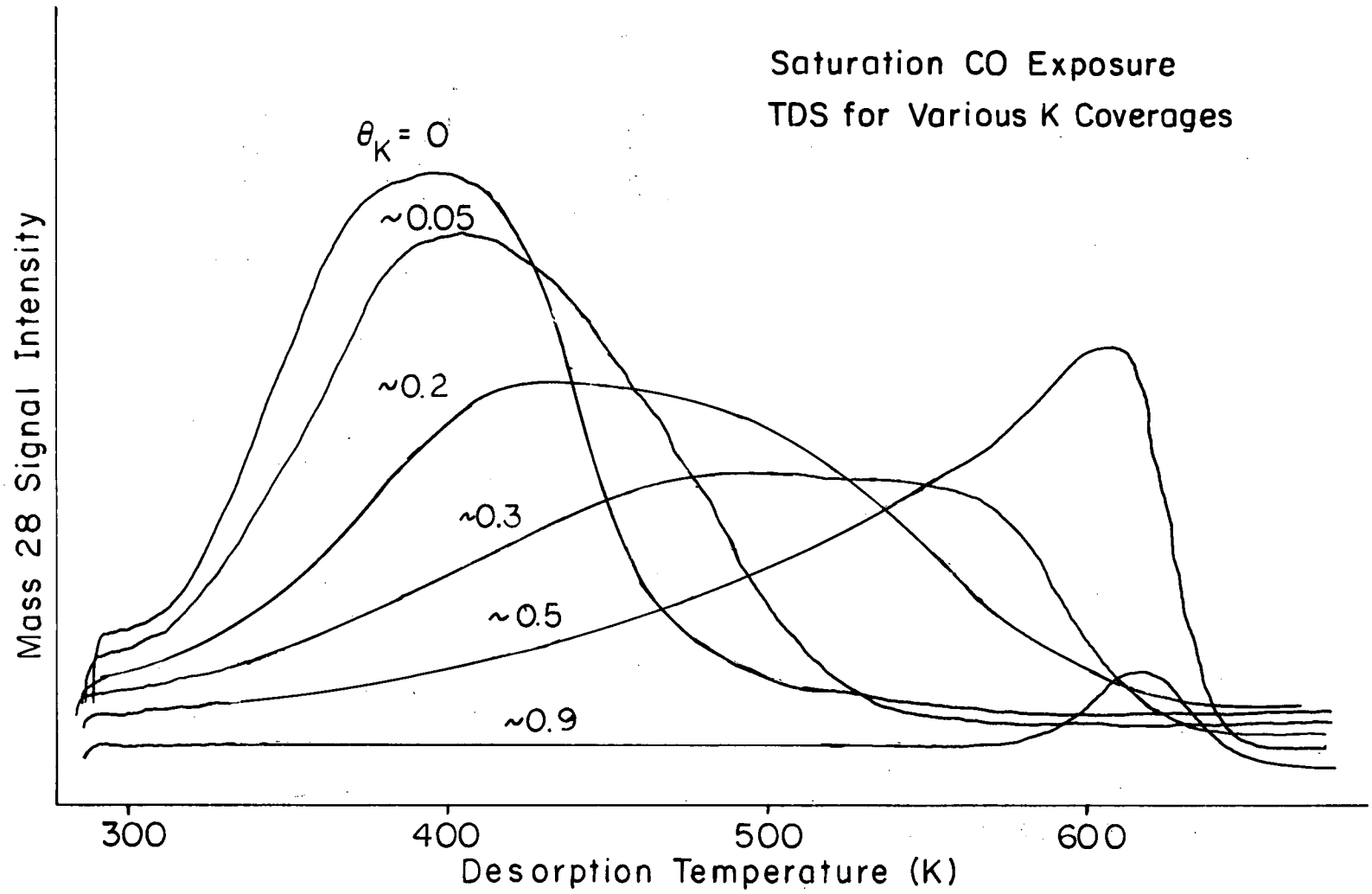

XBL 819-6461B

Fig. 23

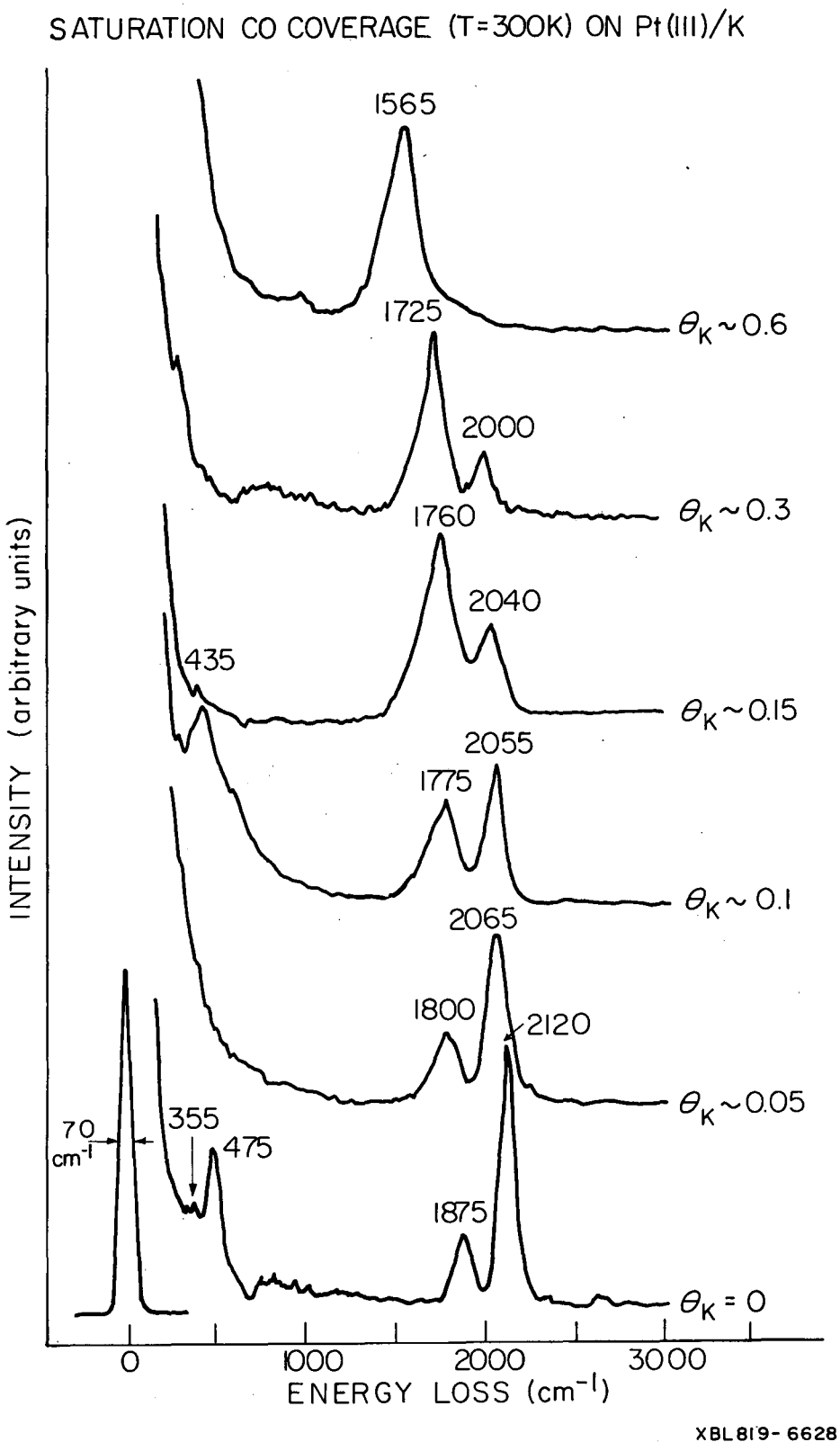
SATURATION CO COVERAGE (T=300K) ON Pt(111)/K
1565
1725
2000
1760
2040
435
2055
1775
2065
1800
2120
355
475
70
cm-1
1875
θK ~ 0.6
θK ~ 0.3
θK ~ 0.15
θK ~ 0.1
θK ~ 0.05
θK = 0
INTENSITY (arbitrary units)
0
1000
2000
3000
ENERGY LOSS (cm-1)
XBL819-6628

Fig. 24

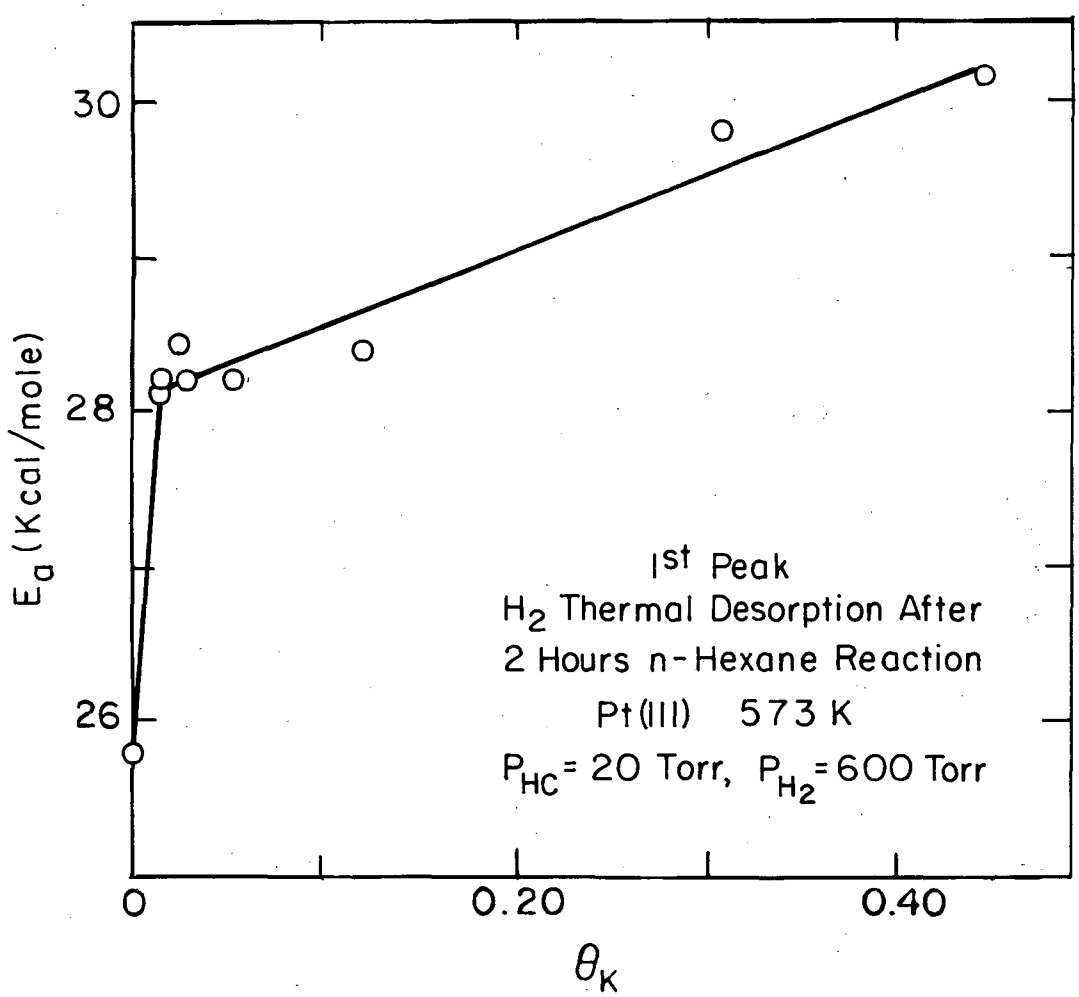

XBL 823-5304 A

Fig. 25

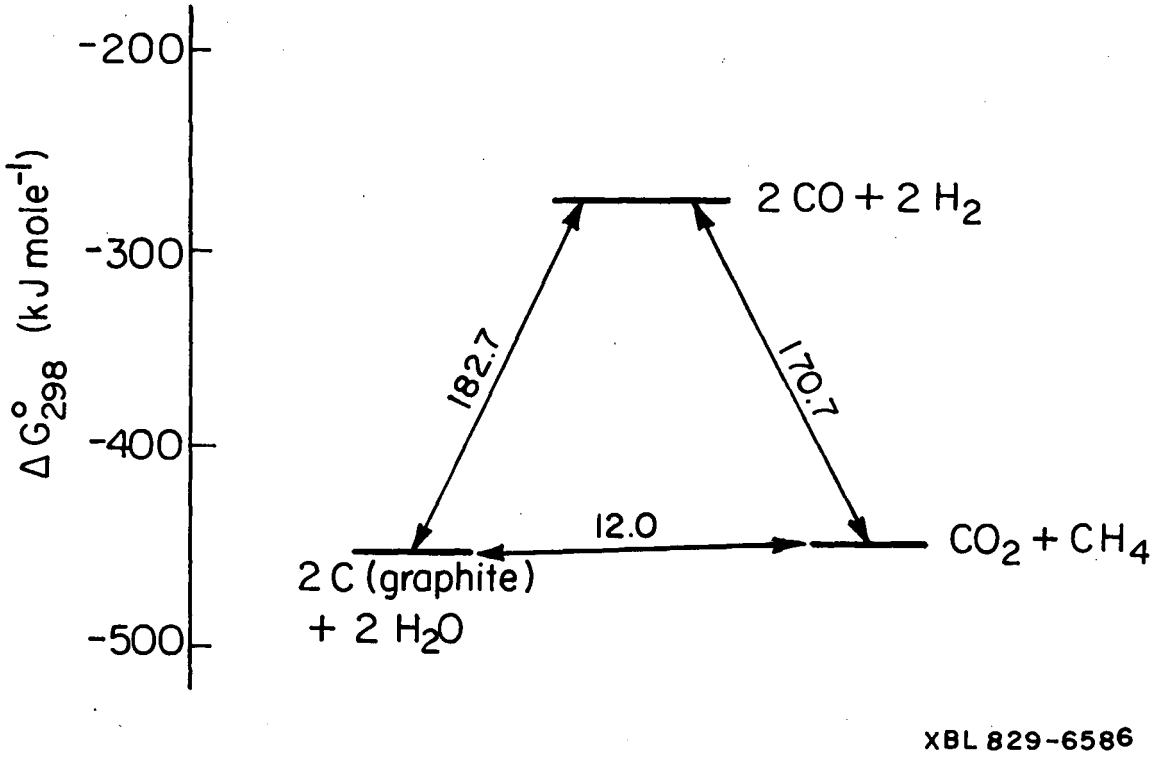
-200
-300
-400
-500
ΔG^{o}_{298} (kJ mole^{-1})
2 CO + 2 H_2
182.7
170.7
12.0
2 C (graphite)
+ 2 H_2O
CO_2 + CH_4
XBL 829-6586

Fig. 26(a)

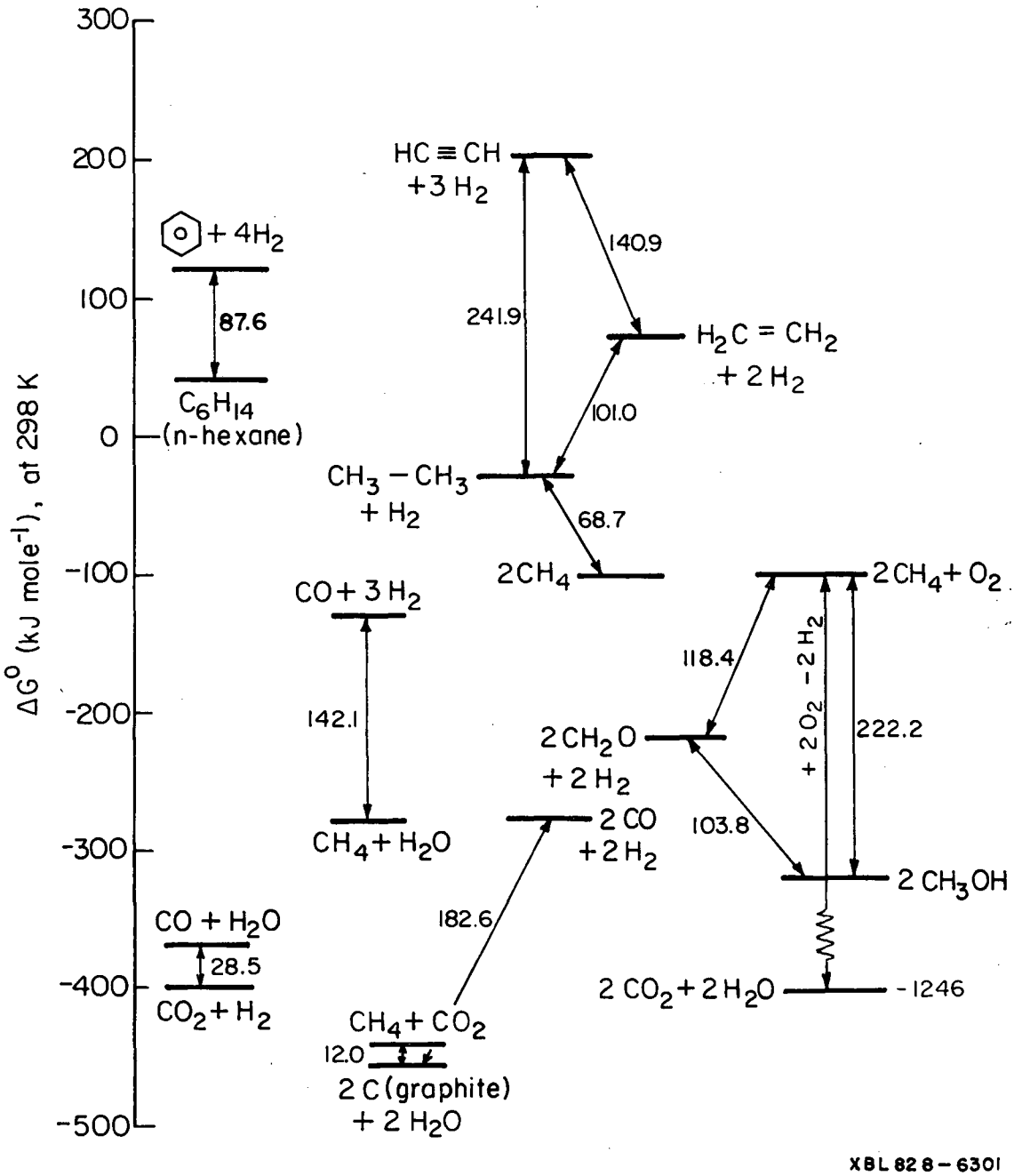
300
200
100
0
-100
-200
-300
-400
-500
ΔG° (kJ mole⁻¹), at 298 K
+ 4H2
87.6
C6H14
(n-hexane)
CO + H2O
28.5
CO2 + H2
HC ≡ CH
+3 H2
140.9
241.9
H2C = CH2
+ 2 H2
101.0
CH3 − CH3
+ H2
68.7
2CH4
CO + 3 H2
142.1
CH4 + H2O
2 CH2O
+ 2 H2
2 CO
+ 2 H2
182.6
CH4 + CO2
12.0
2 C (graphite)
+ 2 H2O
2CH4 + O2
118.4
+ 2 O2 − 2 H2
222.2
103.8
2 CH3OH
2 CO2 + 2 H2O
-1246
XBL 828-6301

Fig. 26(b)

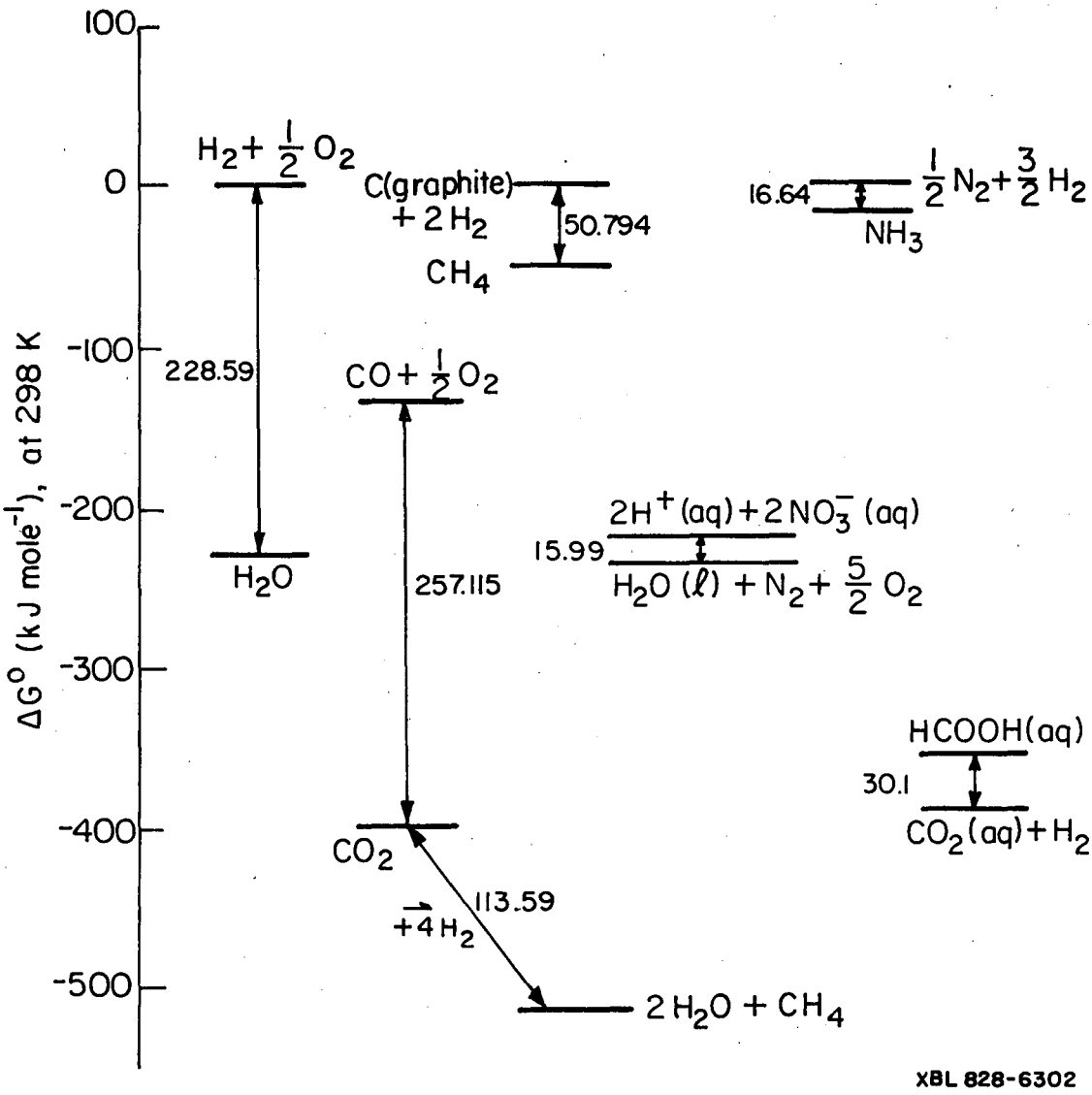
100
0
-100
-200
-300
-400
-500
ΔG° (kJ mole⁻¹), at 298 K
H2 + 1/2 O2
H2O
228.59
C(graphite) + 2 H2
CH4
50.794
CO + 1/2 O2
CO2
257.115
+4 H2
113.59
2 H2O + CH4
16.64
1/2 N2 + 3/2 H2
NH3
2H+(aq) + 2 NO3−(aq)
15.99
H2O (ℓ) + N2 + 5/2 O2
HCOOH(aq)
30.1
CO2(aq) + H2
XBL 828-6302

Fig. 26(c)

This report was done with support from the Department of Energy. Any conclusions or opinions expressed in this report represent solely those of the author(s) and not necessarily those of The Regents of the University of California, the Lawrence Berkeley Laboratory or the Department of Energy.

Reference to a company or product name does not imply approval or recommendation of the product by the University of California or the U.S. Department of Energy to the exclusion of others that may be suitable.

TECHNICAL INFORMATION DEPARTMENT
LAWRENCE BERKELEY LABORATORY
UNIVERSITY OF CALIFORNIA
BERKELEY, CALIFORNIA 94720